

The physics of interstellar photon-dominated regions (PDRs)

Chemistry I+II
(based on lecture notes by E. van Dishoeck, Leiden)

SS 2007

Basic Molecular Processes

Formation processes

radiative association:

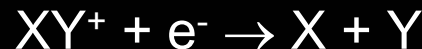
grain surface reaction:



Destruction processes

photodissociation:

dissociative recombination:



Rearrangement processes

ion-molecule reaction:

charge transfer reaction:

neutral-neutral reactions:



Destruction processes

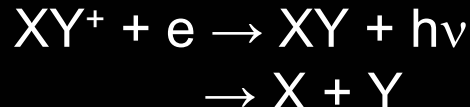
4. Dissociative recombination

atomic ions:



radiative \Rightarrow slow

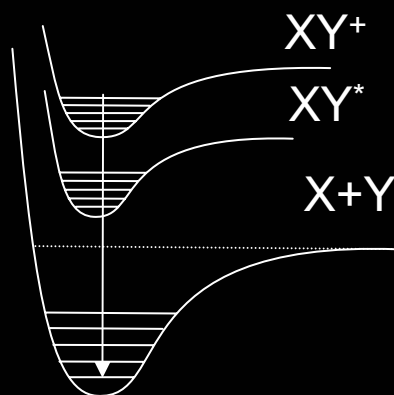
molecular ions:



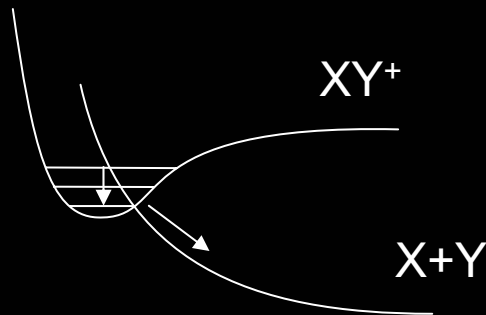
radiative \Rightarrow slow

dissociative \Rightarrow very rapid at low T

energy



slow

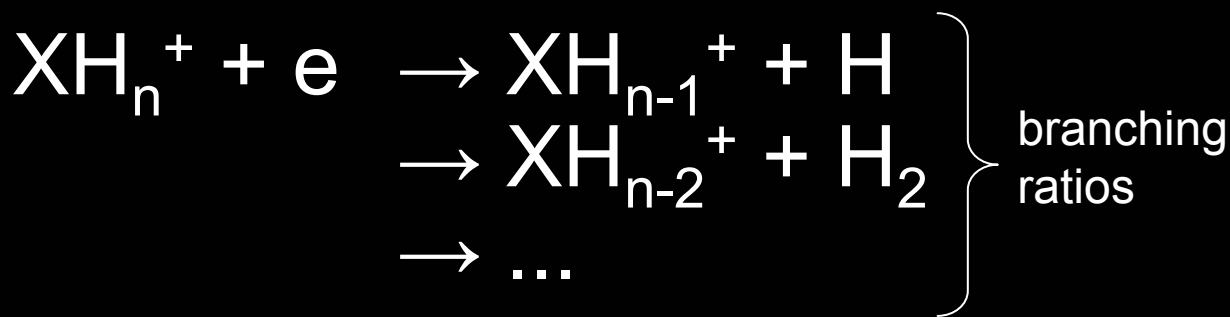


rapid

Need curve crossing between XZ^+ and repulsive XY potential for reaction to proceed fast. Occurs for most molecular ions.

Destruction processes

- major uncertainties in models: products



Example: $H_3O^+ + e^-$	33%	5%
$\rightarrow H_2O + H$	33%	5%
$\rightarrow OH + H_2$	18%	36%
$\rightarrow OH + H + H$	48%	29%
$\rightarrow OH + H_2 + H$	1%	30%

3-body products

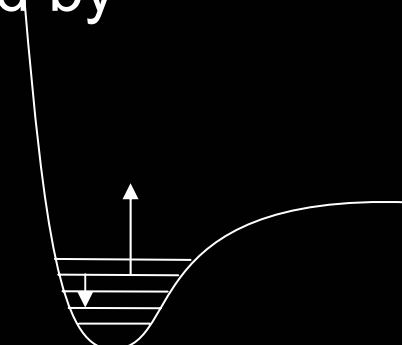
Vejby_C et al. '97

Williams et al. '96

Destruction processes

5. Collision induced dissociation

If T is high enough ($T > 5000K$), H_2 is destroyed by collisions



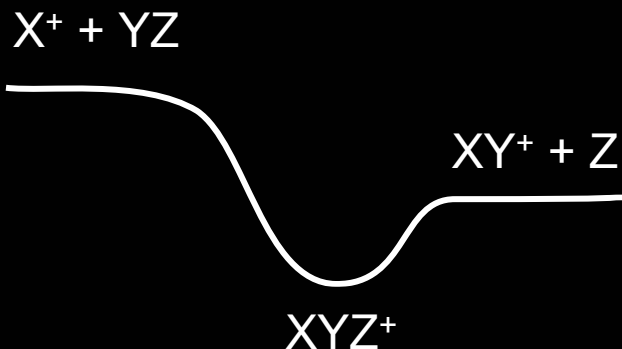
H_2 has no permanent dipole moment \Rightarrow significant population in high v levels at high T \Rightarrow large dissociation rate

CO has small dipole moment \Rightarrow radiative stabilization rapid
 \Rightarrow not much pop. in high v
 \Rightarrow small dissociation rate

Rearrangement processes

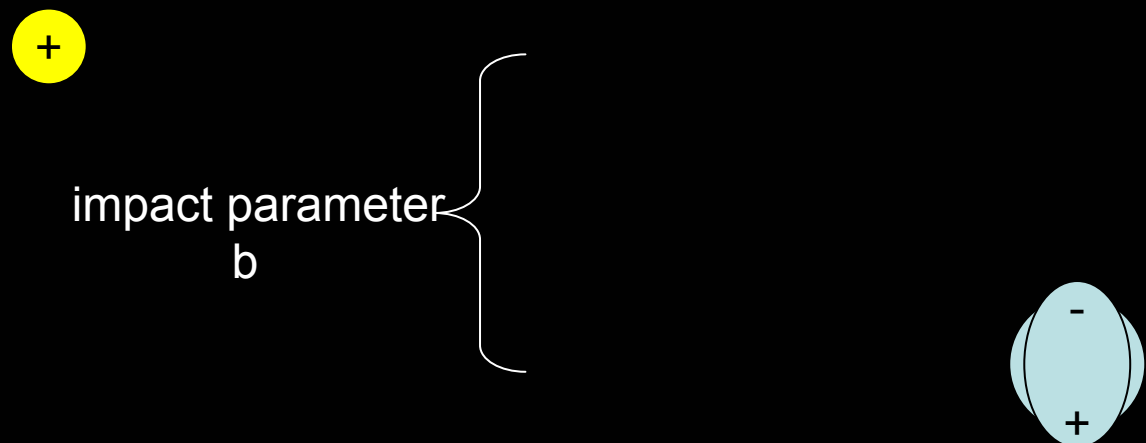
7. Ion-molecule reactions

long-range attraction: ion-(induced) dipole $\sim 1/R^4$
 \Rightarrow rapid at low T if reaction is exothermic



collision energy in ISM ~ 0.01 eV
 \Rightarrow calculation of collision cross section via potential surface
calculation requires high precision

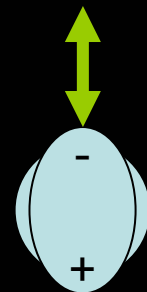
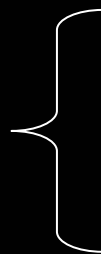
Rearrangement processes



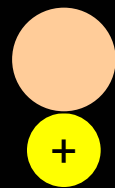
Rearrangement processes



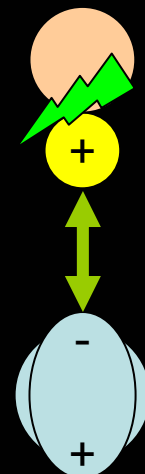
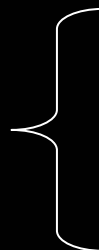
critical impact
parameter b_c



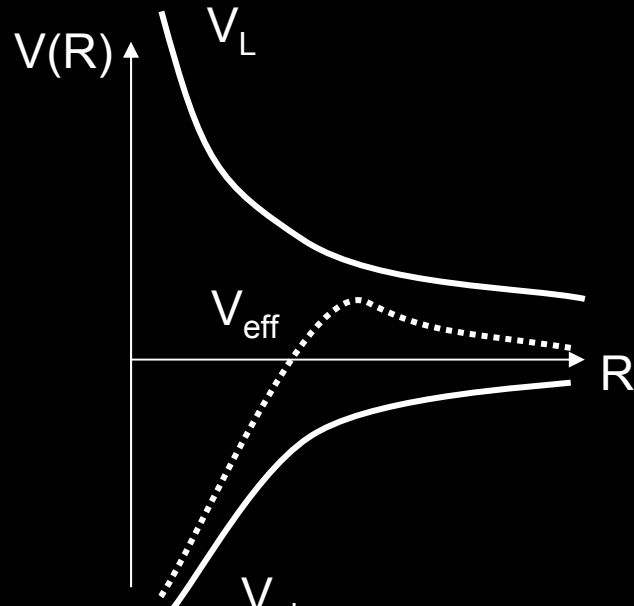
Rearrangement processes



critical impact
parameter b_c



Rearrangement processes



centrifugal potential $V_L = \frac{\mu b^2 v^2}{2R^2}$

ion induced dipole $V_{el} = -\frac{e^2 \alpha}{2R^4}$

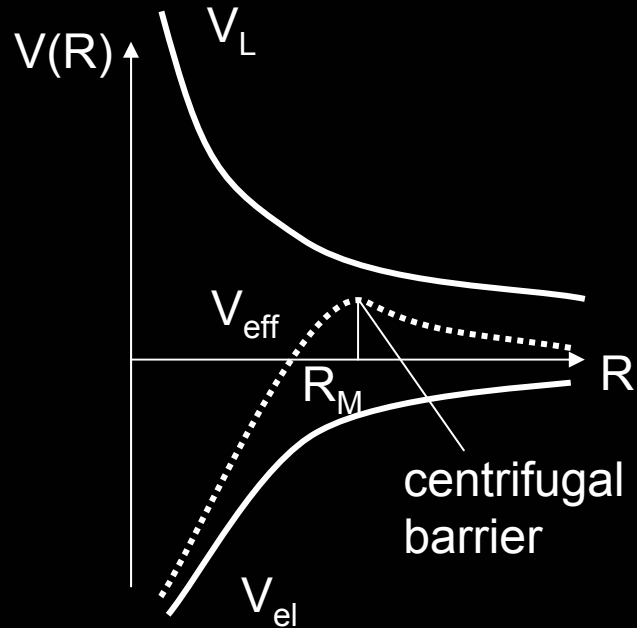
$$V_{eff} = -\frac{e^2 \alpha}{2R^4} + \frac{\mu b^2 v^2}{2R^2}$$

μ : reduced mass

α : polarizability ($\sim 10^{-24} \text{ cm}^3$)

$L = m b v$: angular momentum in centrifugal potential

Rearrangement processes



$$V_{eff} = -\frac{e^2 \alpha}{2R^4} + \frac{\mu b^2 v^2}{2R^2}$$

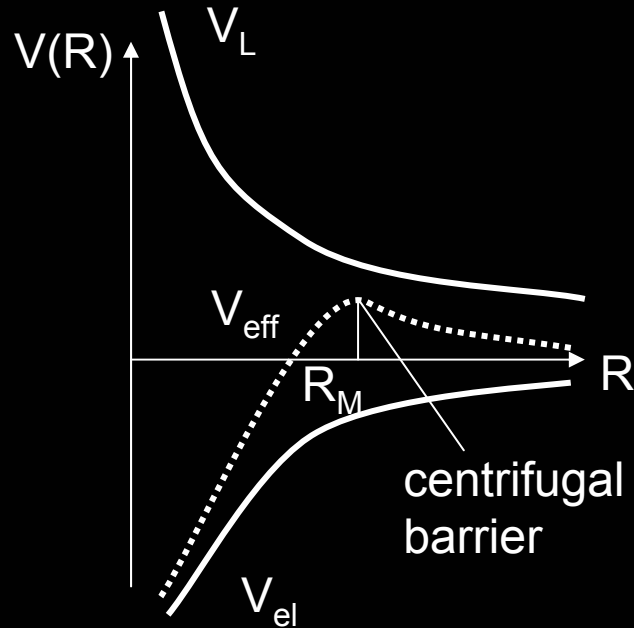
$$\max V_{eff}: \frac{(\mu b^2 v^2)^2}{2\alpha e^2} \quad \text{at} \quad R_M^2 = \frac{2\alpha e^2}{\mu b^2 v^2}$$

barrier can only be surmounted if:

$$\frac{1}{2} \mu v^2 > \frac{(\mu b^2 v^2)^2}{2\alpha e^2}$$

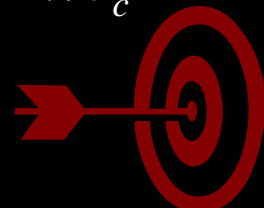
critical impact parameter $b_c = \left(\frac{4\alpha e^2}{\mu v^2} \right)^{1/4}$

Rearrangement processes



critical impact parameter: $b_c = \left(\frac{4\alpha e^2}{\mu v^2} \right)^{1/4}$

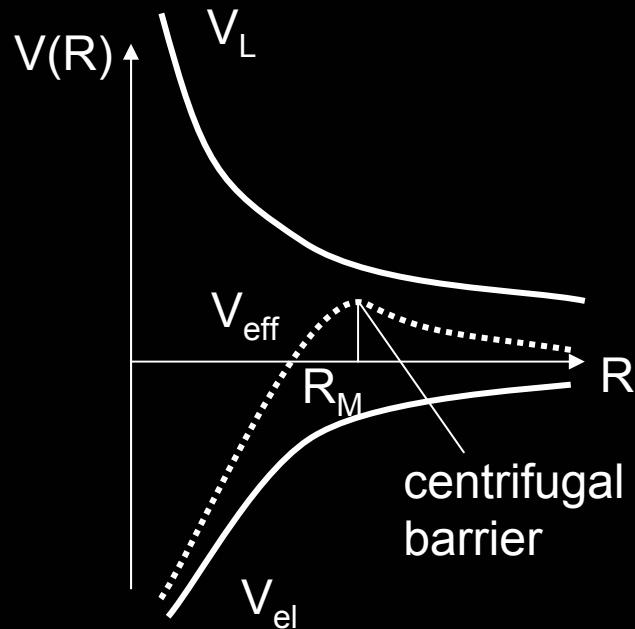
cross section for reaction: $\sigma = \pi b_c^2$



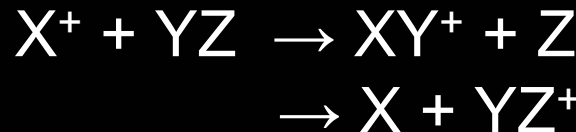
collision frequency: $k = <\sigma v> = 2\pi \left(\frac{\alpha e^2}{\mu} \right)^{1/2}$

$\Rightarrow k \sim 10^{-9} \text{ cm}^3 \text{s}^{-1}$, independent of T!

Rearrangement processes



possible processes:



exchange
charge
transfer

many experiments performed at room T,
some at low T. Most reactions proceed at
Langevin rate, but some exceptions
known!

Rate coefficients for ion-polar molecule reactions may be factors of 10-100 larger than Langevin values at low T, because $V(R) \sim R^{-2}$ (eg. $C^+ + OH \rightarrow CO^+ + H$
 $H_3^+ + CS \rightarrow HCS^+ + H_2$)

Rearrangement processes

- long range attraction: weak van der Waals interaction $\sim 1/R^6$ (Woon & Herbst '97)



μ_1 : dipole moment of CN

α_2 : polarizability of C_2H_2

α_1 : polarizability of CN

I^- : ionization potential

$$V_{el}(R) = -\frac{C_6}{R^6} - \frac{\mu_1^2 \alpha_2}{R^6}$$

dispersion coefficient $C_6 = \frac{3}{2} \frac{I_1 I_2}{I_1 + I_2} \alpha_1 \alpha_2$

Rearrangement processes

- simpler:

$$V_{el}(R) = -\frac{\alpha_1 \alpha_2}{R^6} I$$

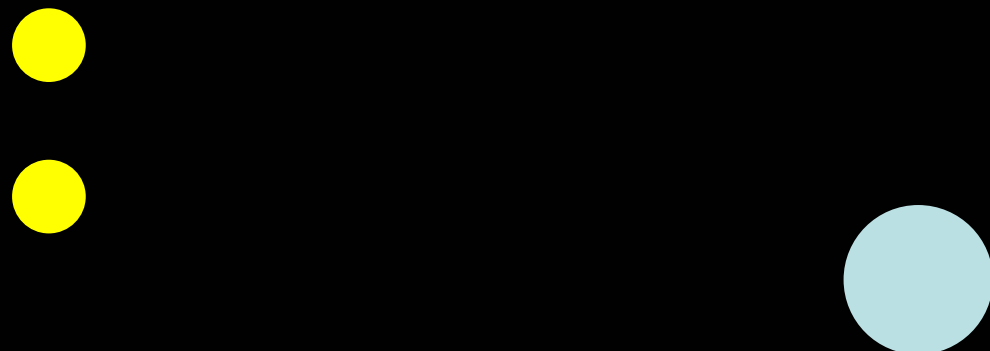
$$k = <\sigma v> \approx \pi \cdot 13.6 \left(\frac{\alpha_1 \alpha_2}{\mu} I \right)^{1/3} < v^{1/3} > \approx 4 \times 10^{-11} \text{ cm}^3 \text{s}^{-1}$$

$$\Rightarrow k_{n-n} \ll k_{i-n}$$

\Rightarrow neutral-neutral reactions
unimportant (exception:
reactions with radicals)

Rearrangement processes

- comparison:
simple hard sphere collision without
electromagnetic interaction



Rearrangement processes

- comparison:

simple hard sphere collision without
electromagnetic interaction

(Bohr's radius: $r = 5.3 \times 10^{-11} \text{ m} = 5.3 \times 10^{-9} \text{ cm}$)

$$R \approx 10^{-10} \text{ m} = 10^{-8} \text{ cm}$$

$$\Rightarrow \sigma = R^2\pi = 3 \times 10^{-16} \text{ cm}^2, v \approx 10^4 \text{ cm/s}$$

$k = \sigma v$	$\approx 3 \times 10^{-12}$	cm^3s^{-1}	Factor ≈ 1000
$k_{\text{ion-neutral}}$	$\approx 10^{-9}$	cm^3s^{-1}	
$k_{\text{neutral-neutral}}$	$\approx 4 \times 10^{-11}$	cm^3s^{-1}	Factor ≈ 10

Rearrangement processes

Comparison of effective cross section and radii
(assumption: $v=10^4 \text{ cm s}^{-1}$)

$$\sigma = \frac{k}{v}$$

$$r = \sqrt{\frac{\sigma}{\pi}}$$

		$\sigma [\text{cm}^2]$	$r [\text{cm}]$
	hard sphere	3×10^{-16}	10^{-8}
	ion-neutral	10^{-13}	2×10^{-7}
	neutral-neutral	4×10^{-15}	4×10^{-8}

- dipole induction enlarges the effective target radius by a factor of 20 !
- van der Waals induction enlarges r_{eff} by ~ 4

Rearrangement processes

- Adiabatic capture approximation (AC)
 - if collision energy < $V_{\text{eff}}(R)$ \Rightarrow react. prob=0
 - if collision energy > $V_{\text{eff}}(R)$ \Rightarrow react. prob=1

(ignores angular dependencies, short range effects, quantum effects, activation energies)

With AC theory, the rate coefficient is:

$$k(T) \propto T^{-\frac{2}{n} + \frac{1}{2}} \quad \text{as} \quad T \rightarrow 0$$

for potentials of form r^{-n}

Rearrangement processes

$$k(T) \propto T^{-\frac{2}{n} + \frac{1}{2}} \text{ as } T \rightarrow 0, \text{ for potentials of form } r^{-n}$$

interaction		low T dependence
charge-induced dipole	r^{-4}	T^0
charge-dipole	r^{-2}	$T^{-1/2}$
charge-quadrupole	r^{-3}	$T^{-1/6}$
dipole-dipole	r^{-3}	$T^{-1/6}$
dipole-quadrupole	r^{-4}	T^0
dispersion	r^{-6}	$T^{1/6}$

neutral-neutral reactions typically factor 5 smaller than ion-molecule reactions at low T

Time scales

rate coefficient : k [cm³ s⁻¹]

rate : $k n_A n_B$ [cm⁻³ s⁻¹]

reaction time : $t \approx (k n)^{-1}$ [s⁻¹]

Time scales



$$\rightarrow t = 10^{17} \frac{1}{n} \text{s}$$

$$t_{n=10^4} = 10^{13} \text{s} \triangleq 3 \times 10^5 \text{ yr}$$

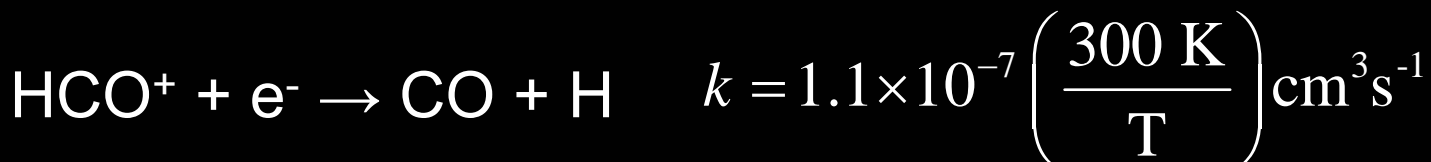


$$\rightarrow t = 5 \times 10^9 \text{s}$$

$$t_{n=10^4} = 160 \text{ yr}$$

Time scales

diss.



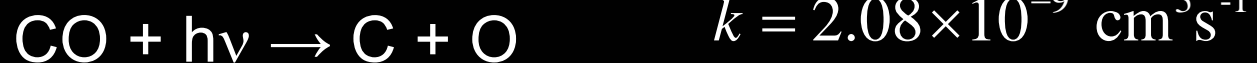
recomb.

$$k_{T=15K} = 2.2 \times 10^{-6} \text{ cm}^3 \text{s}^{-1}$$

$$\rightarrow t = 4.6 \times 10^5 \frac{1}{n_e} \text{s}$$

$$t_{n_e=1} \approx 5 \text{ d}$$

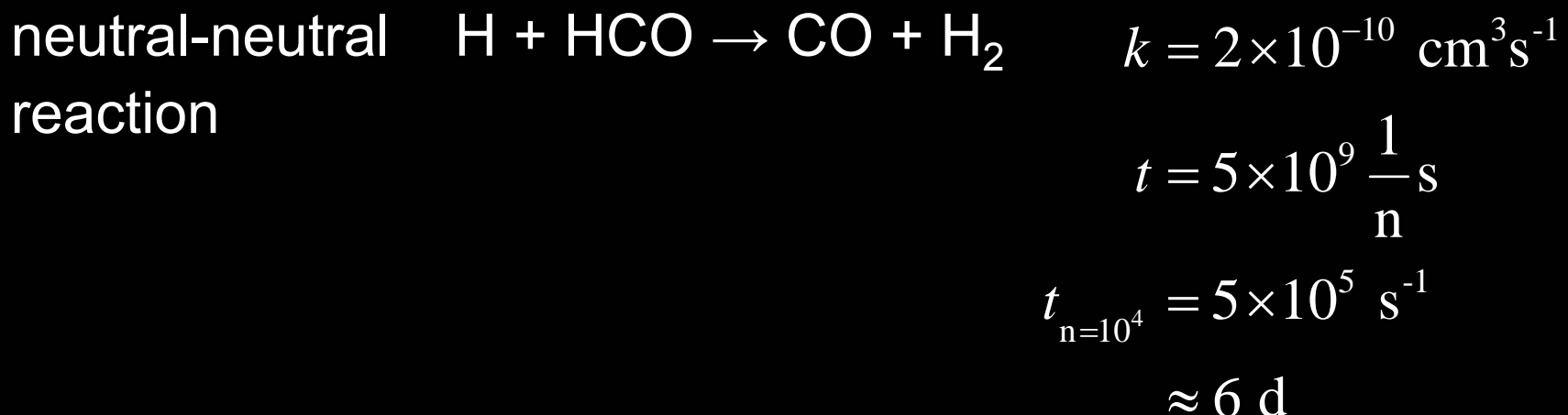
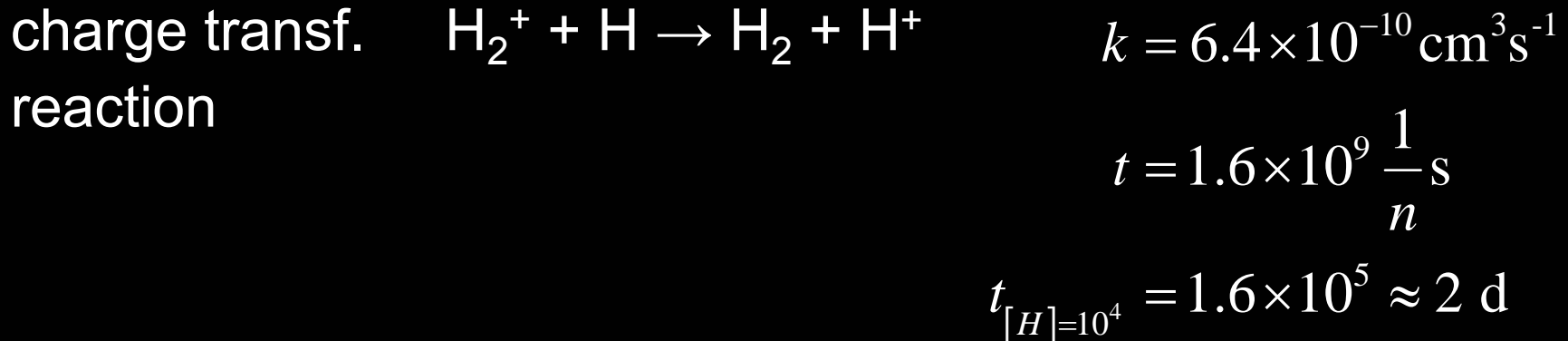
ion-molecule
reaction



$$t = 4.8 \times 10^8 \frac{1}{[\text{H}_2]} \text{s}$$

$$t_{[\text{H}_2]=10^4} = 4.8 \times 10^4 \text{ s}^{-1}$$
$$\approx 0.5 \text{ d}$$

Time scales

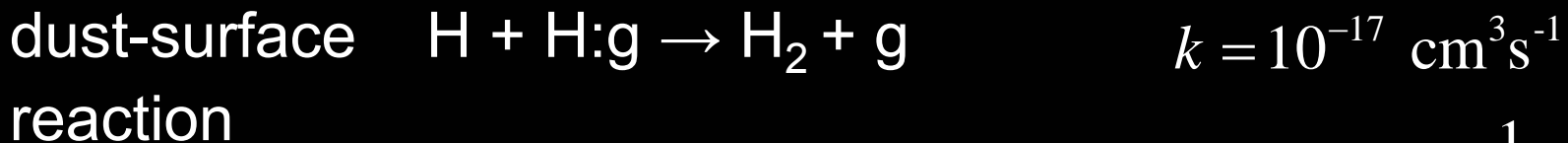


Time scales



$$t = 10^{17} \frac{1}{n} \text{ s}$$

$$t_{[H]=10^4} = 10^{13} \text{ s} \approx 3.2 \times 10^5 \text{ yr}$$



$$t = 2.7 \times 10^9 \frac{1}{n} \text{ yr}$$

$$t_{n=10^4} = 2.7 \times 10^5 \text{ yr}$$

Time scales

Example: ratio H₂/H

$$\frac{d}{dt} [H_2] = -k_{diss} [H_2] + k_{form} [H] \stackrel{!}{=} 0$$

$$\frac{[H_2]}{[H]} = \frac{k_{form}}{k_{diss}} = \frac{t_{diss}}{t_{form}} = \frac{634 \text{ yr}}{2.7 \times 10^9 \text{ yr}} \cdot n = 2.4 \times 10^{-7} n \text{ cm}^{-3}$$

- ⇒ all hydrogen is atomar, unless FUV is attenuated
but: H₂ is detected
- diffuse clouds: [H₂]/[H] ≈ 1
dense clouds: [H₂]/[H] >> 1
- ⇒
- dust extinction
 - self shielding

Degree of Ionization

- electron production:



radiative recombination of atomic ions too slow

⇒ charge exchange from H^+, He^+ → molecular ions ($10-100 \text{ } 1/n \text{ yr cm}^{-3}$)

followed by dissociative recombination of molecular ions ($0.3 \text{ } 1/n_e \text{ yr cm}^{-3}$)

Degree of Ionization

$$\frac{d}{dt} [\text{mol.ions}] = -\frac{1}{t_{diss.rec.}} [\text{mol.ions}] + \xi [\text{He}]^! = 0$$

$$= -\frac{1}{0.3 \text{ yr cm}^{-3}} n_e^2 + \xi \frac{1}{10} n = 0$$

$$n_e \approx 10^{-4} \text{ cm}^{-3} \sqrt{n}$$

$$t_{diss.rec.} \approx 3 \times 10^3 \text{ yr} \sqrt{\frac{1}{n}}$$

compared to:

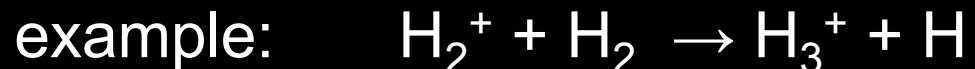
exchange reactions $t \approx 10^{-3} \dots 10^{-2} \text{ yr}$ $1/n$

rad. associations $t \approx 10^4 \text{ yr}$ $1/n$

⇒ many other reactions occur before 1 dissociation/recombination destroys ions/electrons

Degree of Ionization

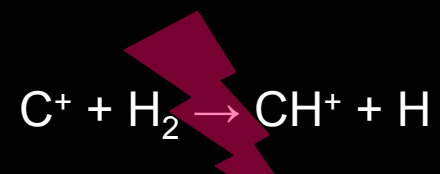
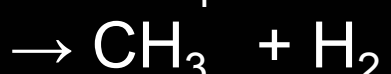
⇒ Ion – Molecule – Scheme:



...

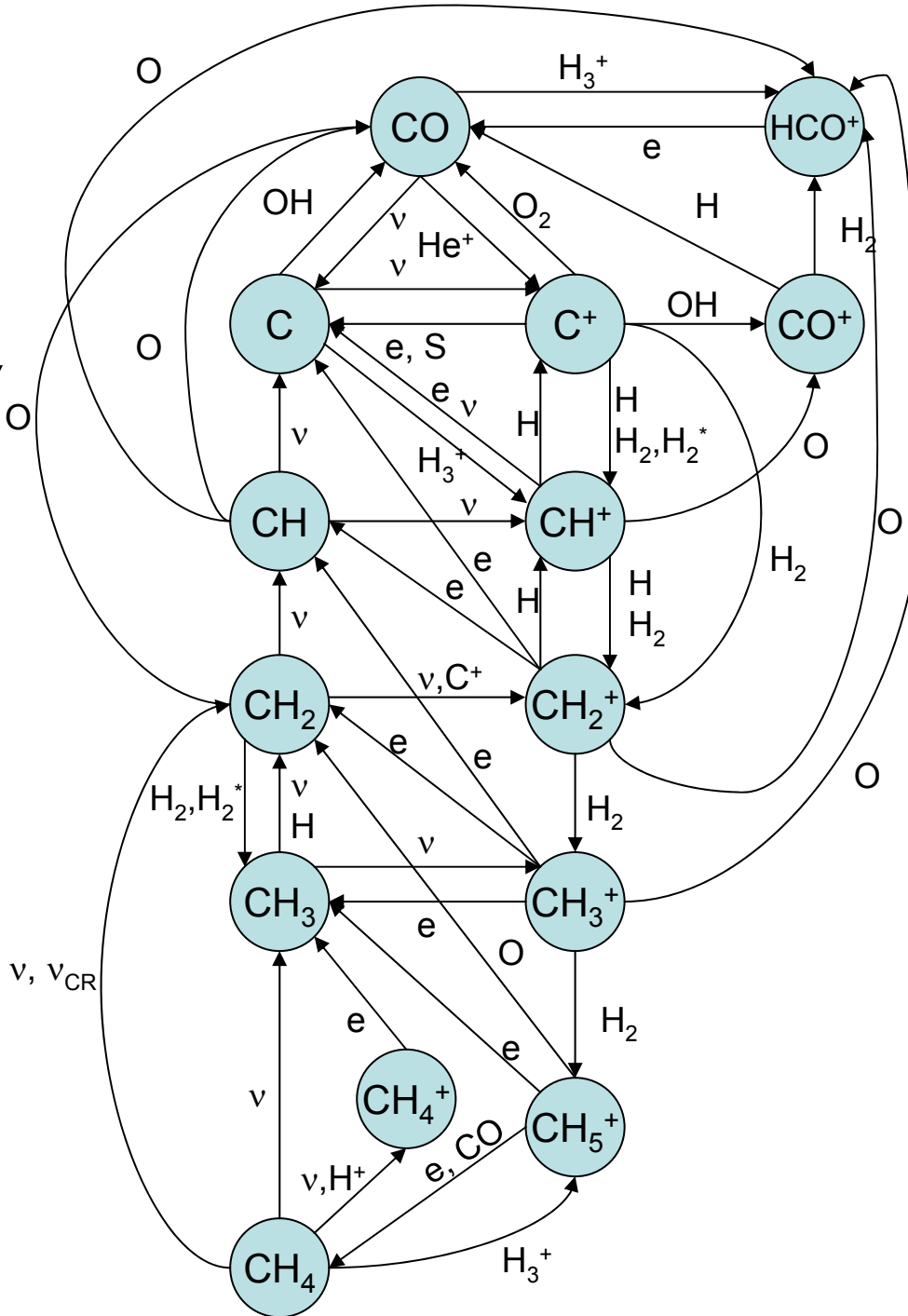
Degree of Ionization

⇒ Ion – Molecule – Scheme:



The carbon roadmap

- Like any roadmap, this network describes *how to get from A to B*.
 - Like on any roadmap, *some paths are quick some are slow*.
 - Unlike any normal roadmap some *slow paths may become very quick under certain conditions*



Example: Diffuse Cloud

starting point: C^+

collision with H_2 :

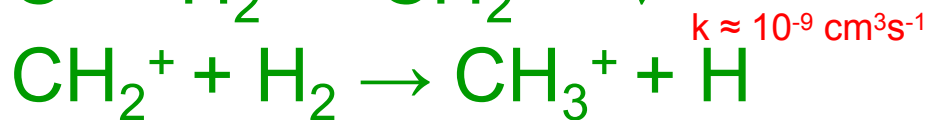


$\Delta E = 4600\text{K}$

instead:



$k \approx 10^{-15} \text{ cm}^3\text{s}^{-1}$



$k \approx 10^{-9} \text{ cm}^3\text{s}^{-1}$

then:

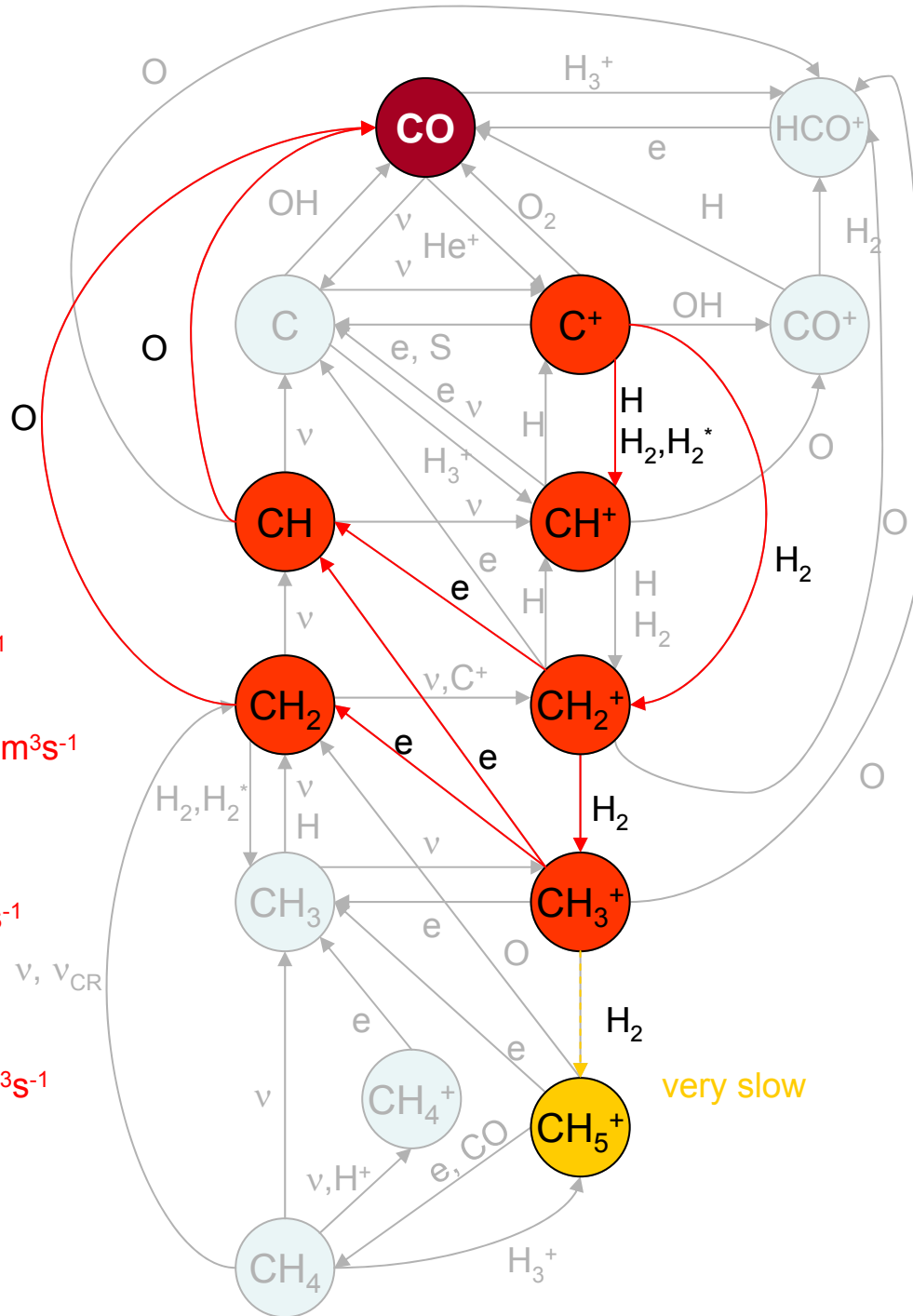


$k \approx 10^{-7} \text{ cm}^3\text{s}^{-1}$

and:



$k \approx 10^{-10} \text{ cm}^3\text{s}^{-1}$

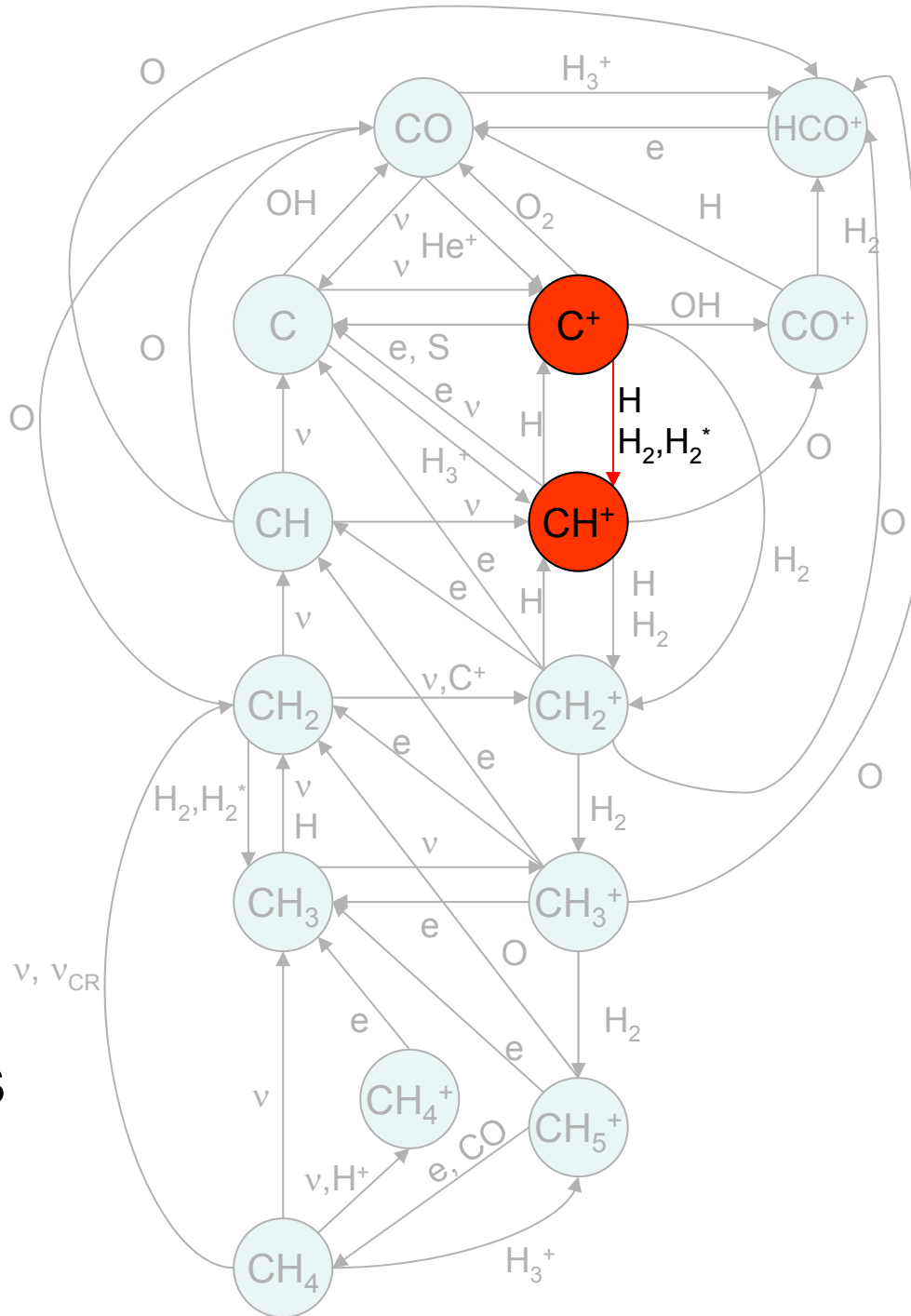


Example: PDR

high FUV intensity heats
the gas at the surface
→ some slow routes
become quick



endothermic reactions
become possible
activation energy barriers
become surmountable



Example: Dark Cloud

cold and dense:

$T=10 \text{ K}$, $n=10^4-10^5 \text{ cm}^{-3}$

carbon locked in CO



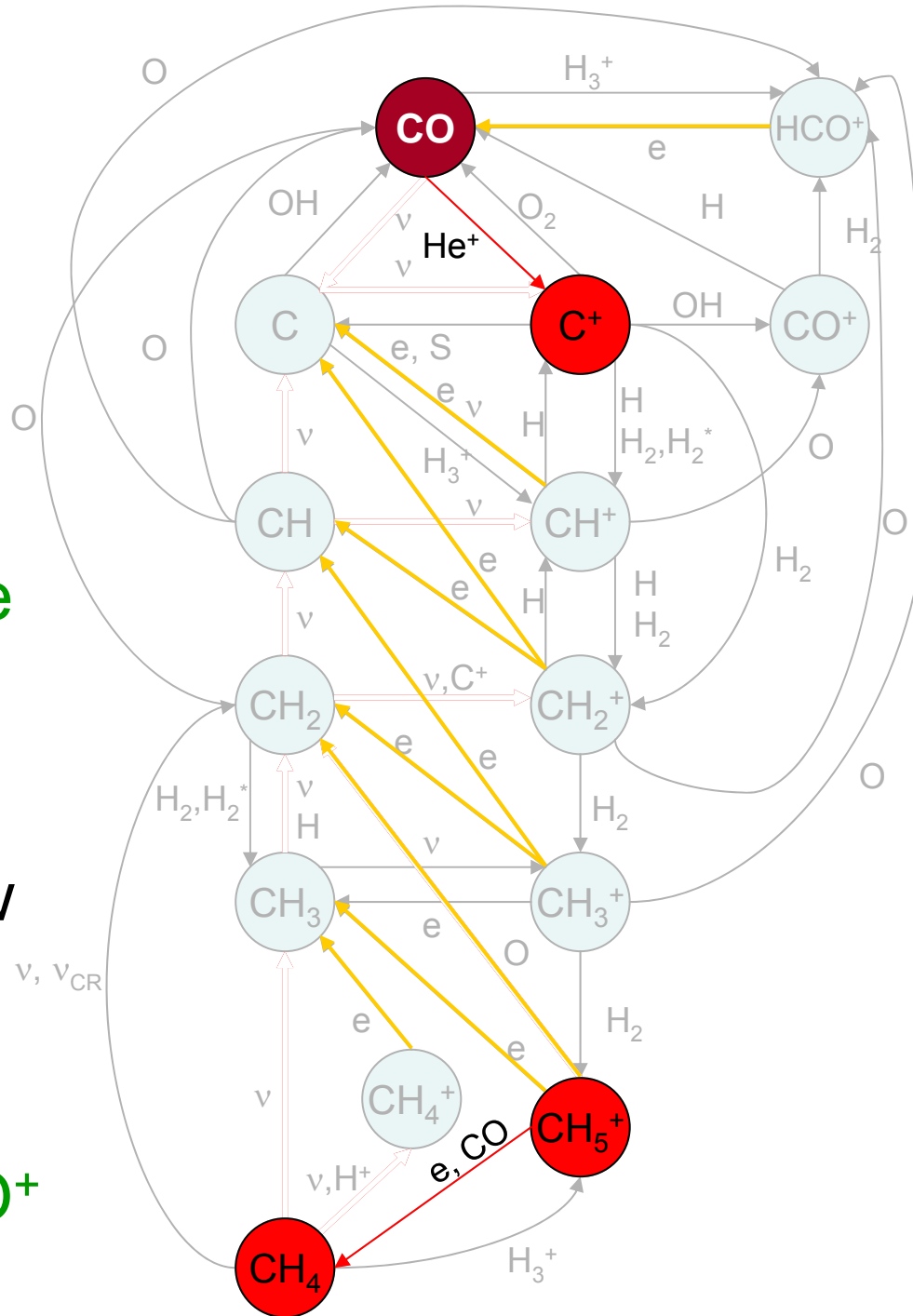
FUV fully absorbed

some roads vanish

some roads become slow

e.g. reactions with e^-

but:

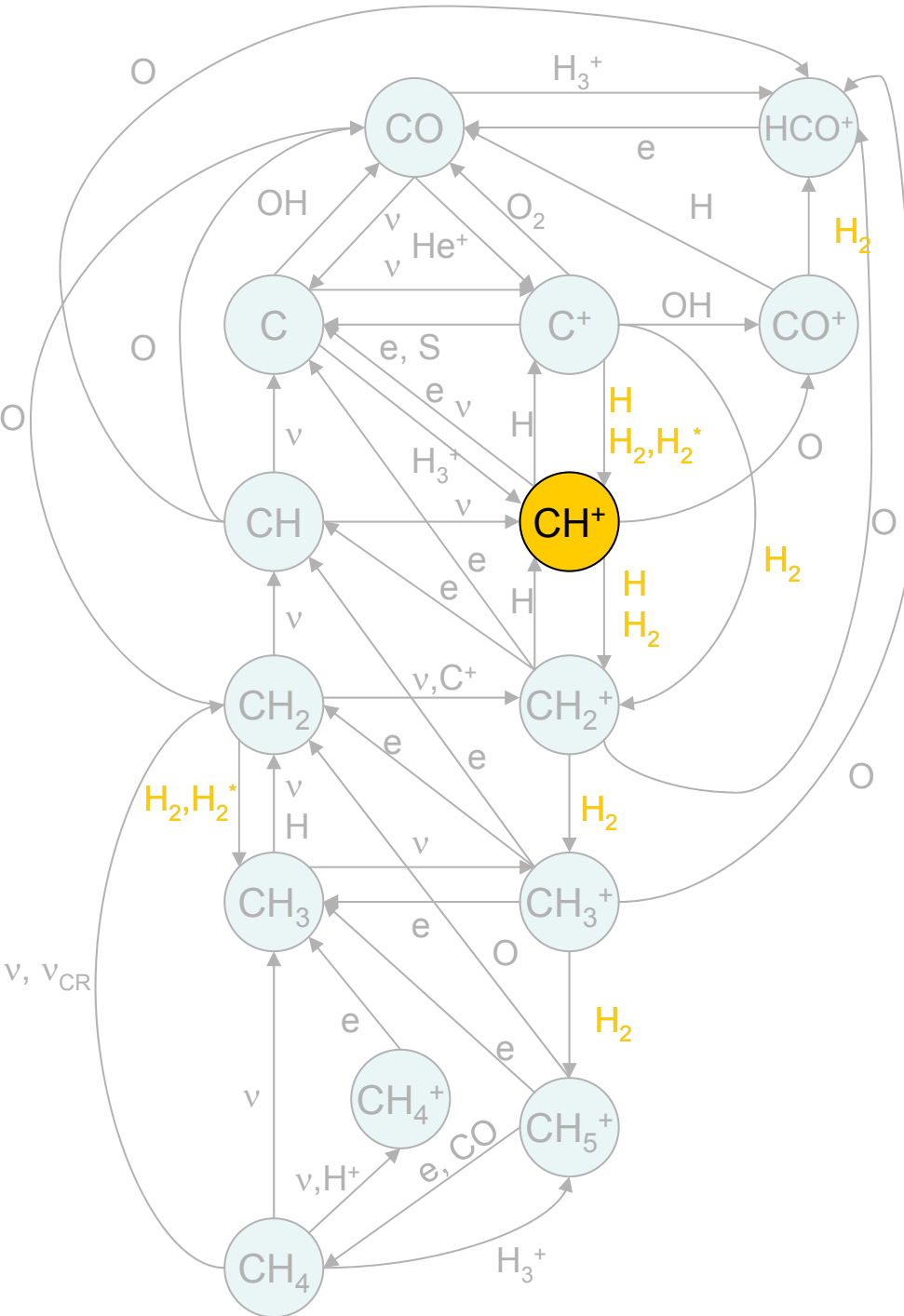


Looks ‘simple’, but:

CH⁺ a factor 100 too low

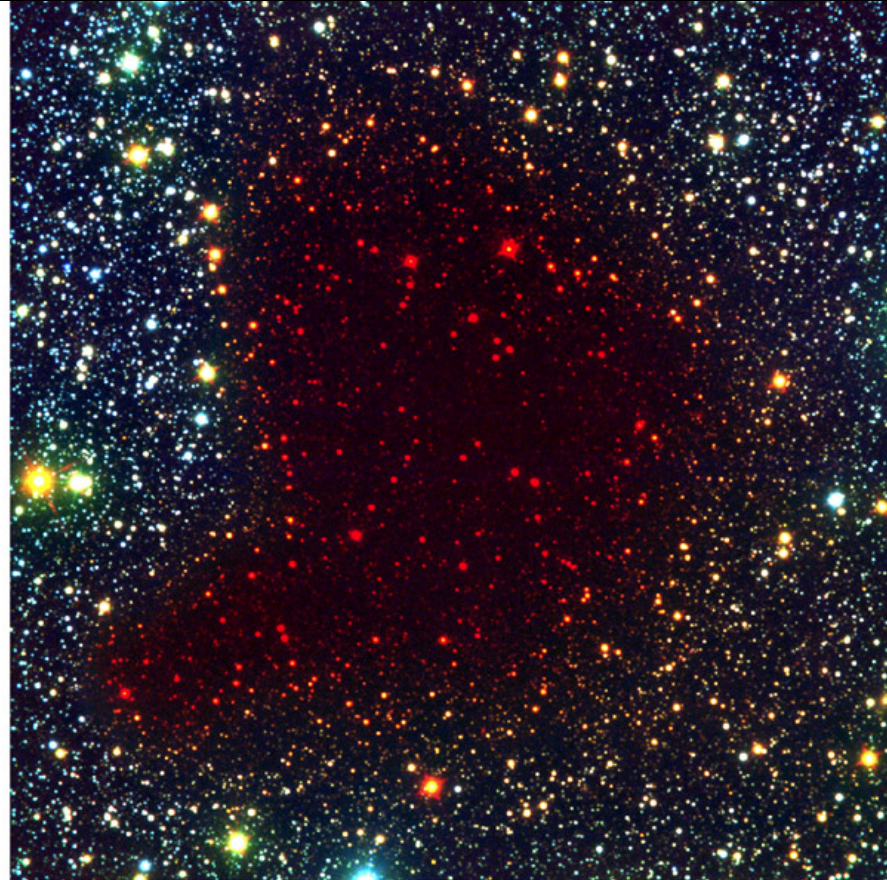
H_2 formation not fully understood

10





B, V, I



B, I, K

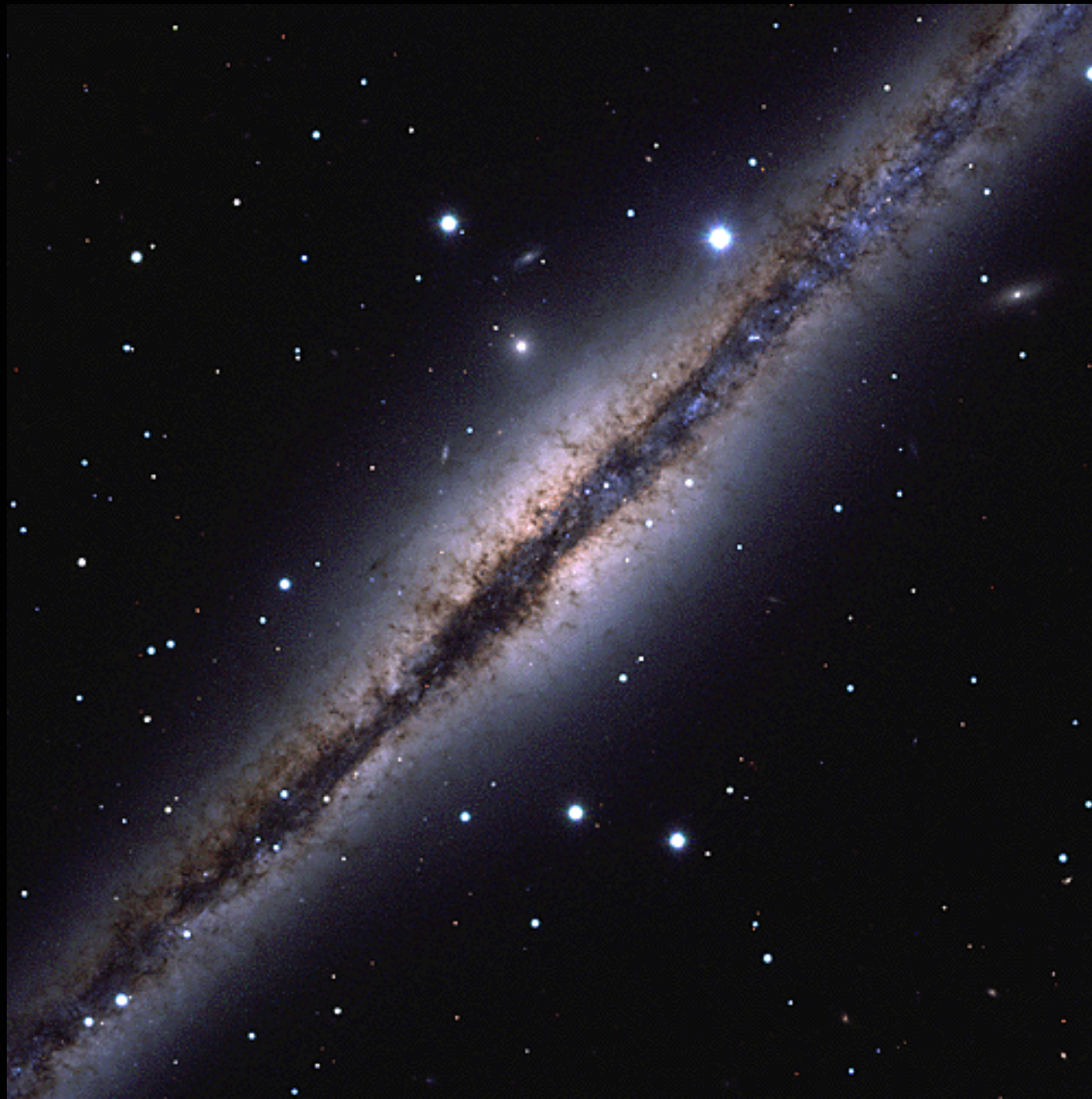
Pre-Collapse Black Cloud B68 (comparison)
(VLT ANTU + FORS 1 - NTT + SOFI)

ESO PR Photo 02c/01 (10 January 2001)

© European Southern Observatory

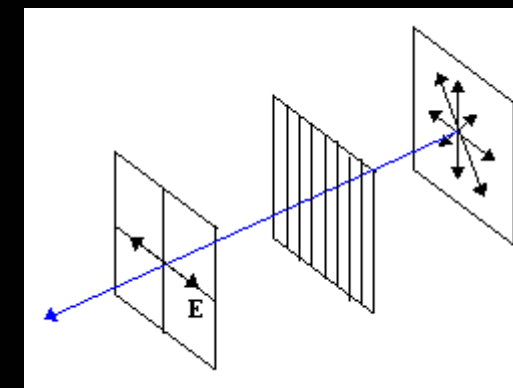
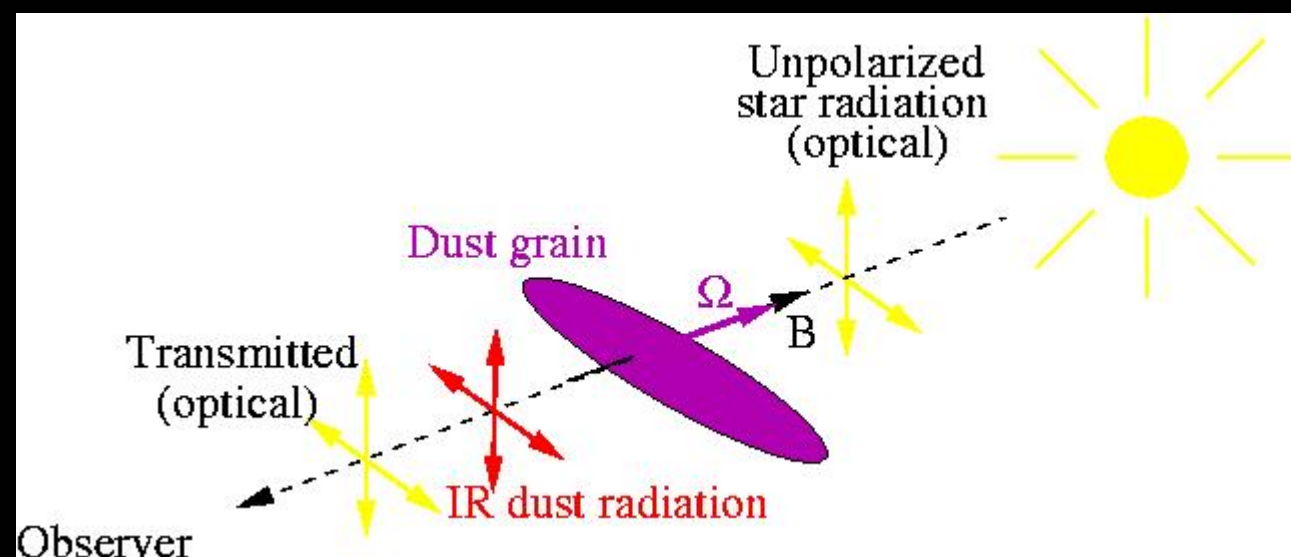
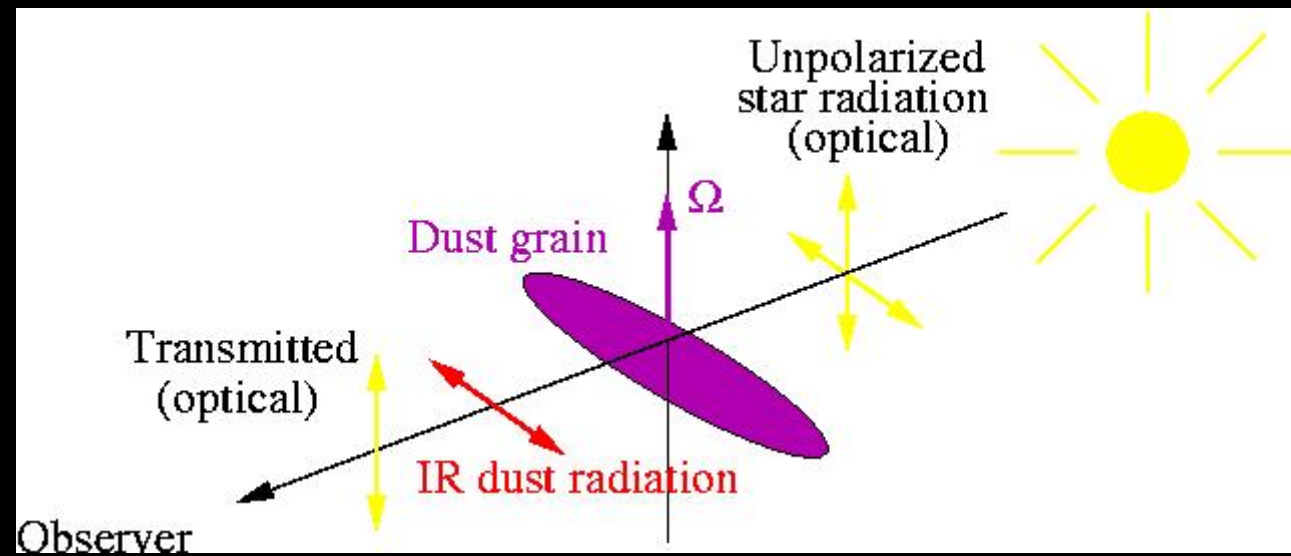


Dust



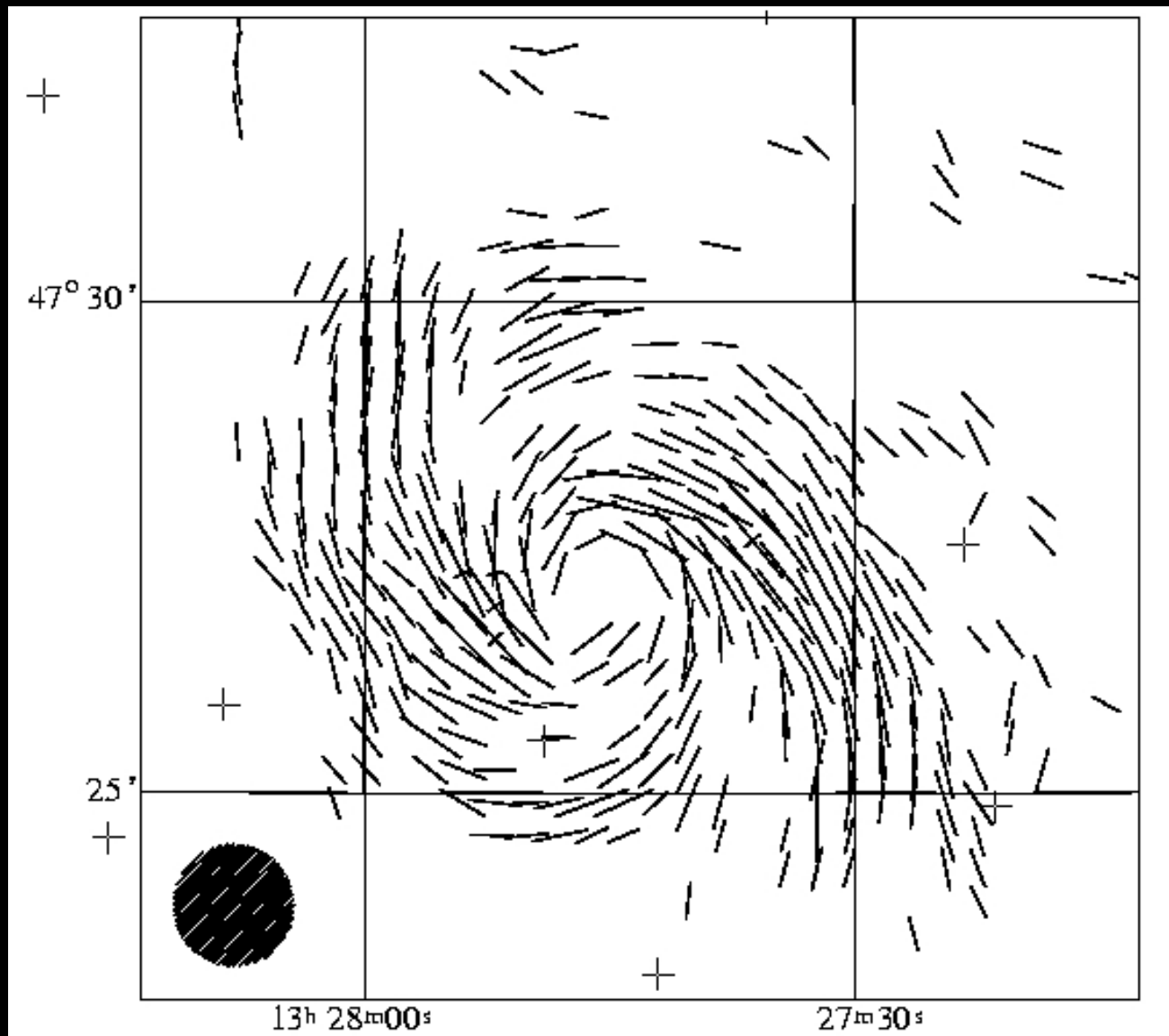
NGC 891

Dust

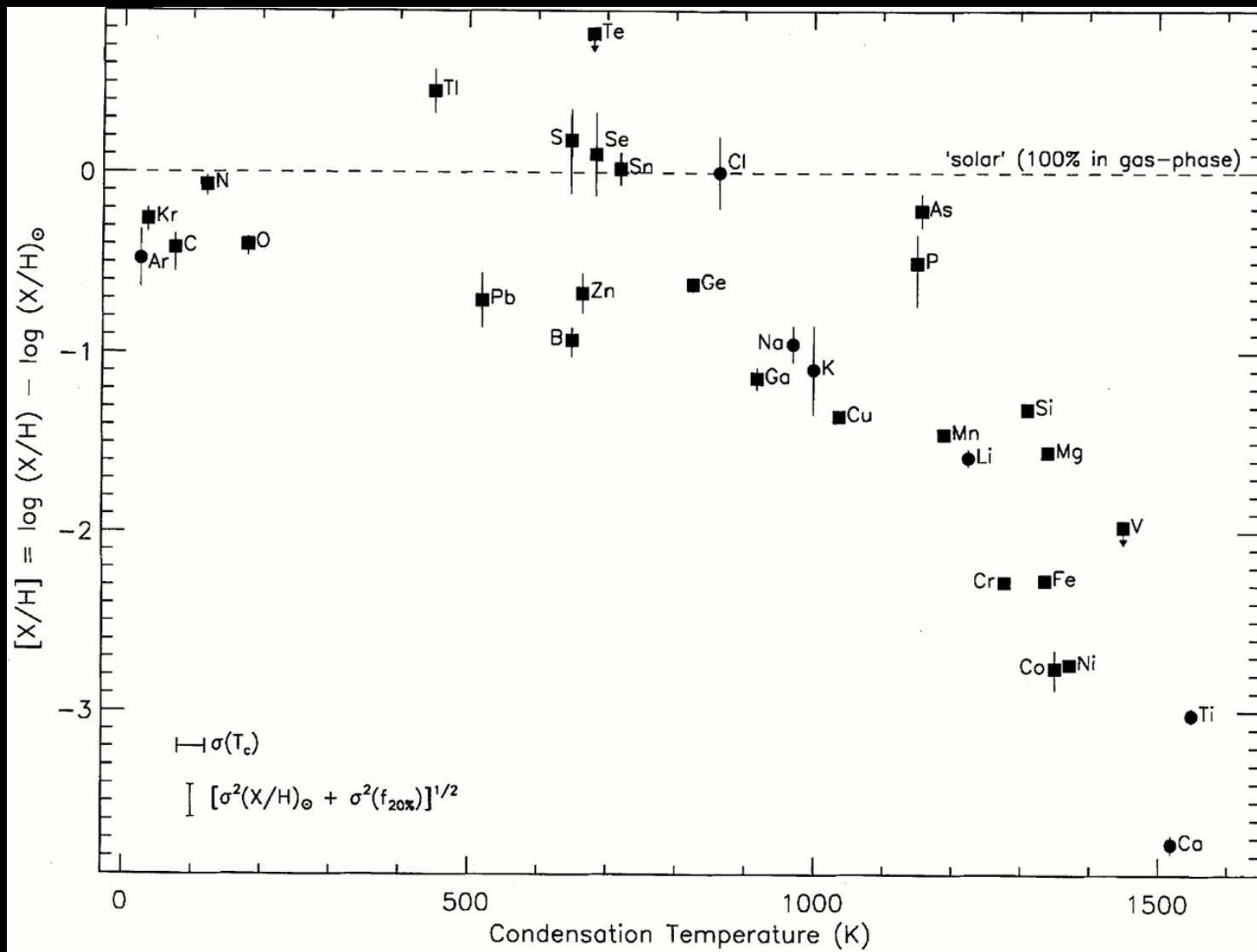


Davis Greenstein
Effect

Dust

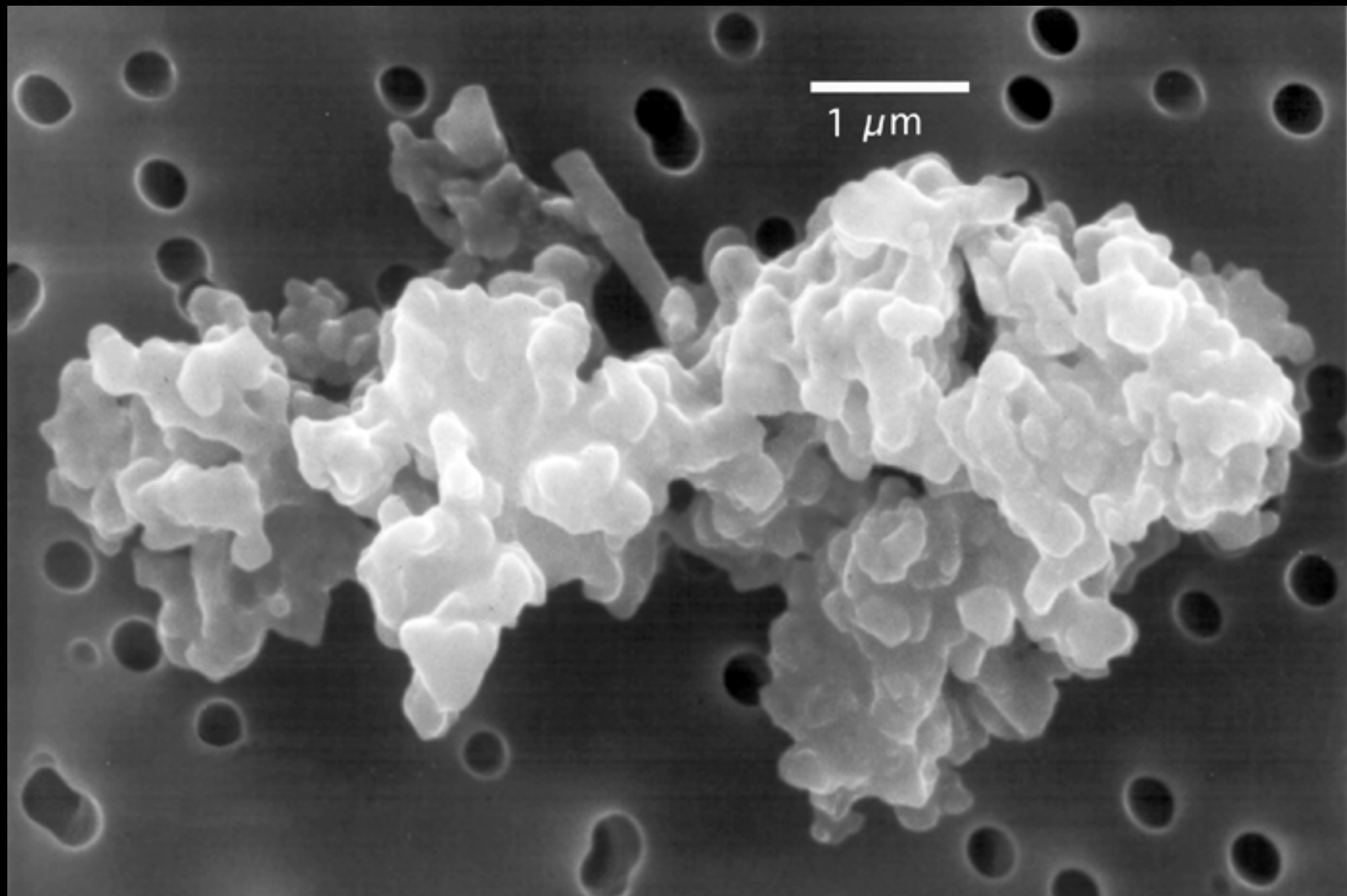


Magnetic field orientation in the Galaxy M51 (Berkhuijsen et al. 1975).



Elemental depletions as a function of condensation temperature (the temperature at which 50% of element condenses out in solid form)

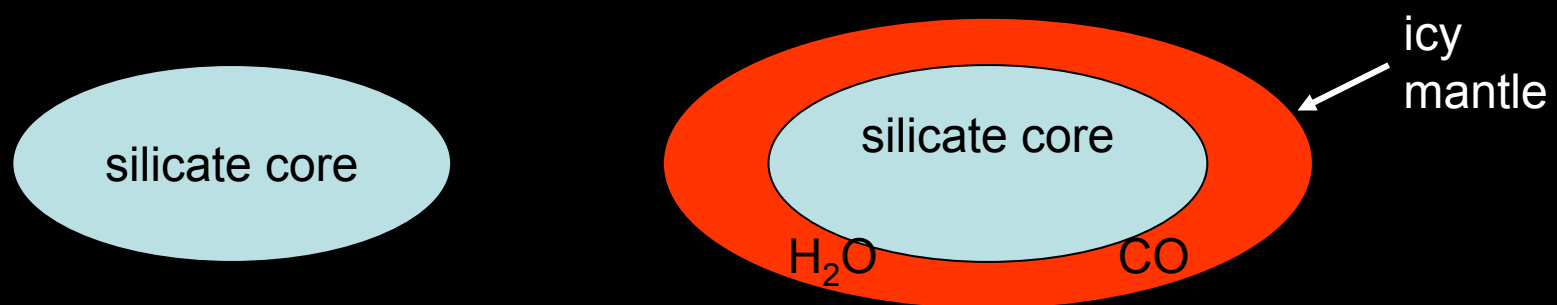
Dust

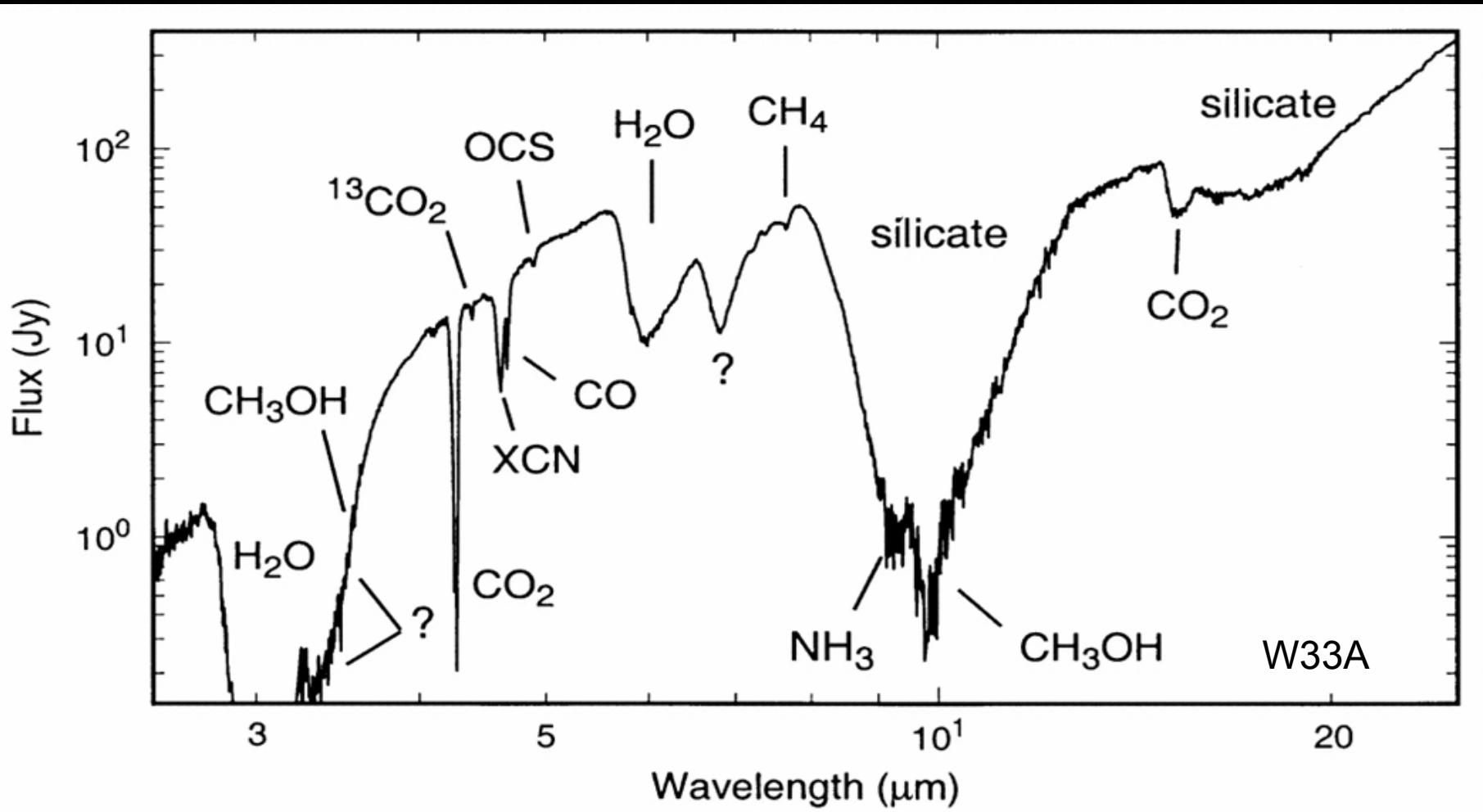


Dust

What is this dust composed of?

- amorphous silicates
 - observed depletion: most of Si, Mg, Fe, and 20% of O is contained in silicates (e.g. MgFeSiO_4 , i.e. Olivine)
 - shape of $9.7\mu\text{m}$ Si_O stretch and $18\mu\text{m}$ O_Si_O bending modes (Gillel & Forrest, '79), absorption features
 - optical extinction + polarization \Rightarrow typical size $\sim 0.1\mu\text{m}$, elongated
 - wavelength dependence of extinction \Rightarrow size distribution, e.g. $n(a) \sim a^{-3.5}$ 50Å-2500Å (MRN)





Dust

- crystalline silicates
 - discrete, relatively sharp emission features found in spectra of old (post) AGB stars, PNe, and young stars with circumstellar disks, but not in ISM! (photons and ions tend to destroy lattice order)
 - features can be identified with Mg-rich crystalline silicates, e.g.



fosterite



enstatite

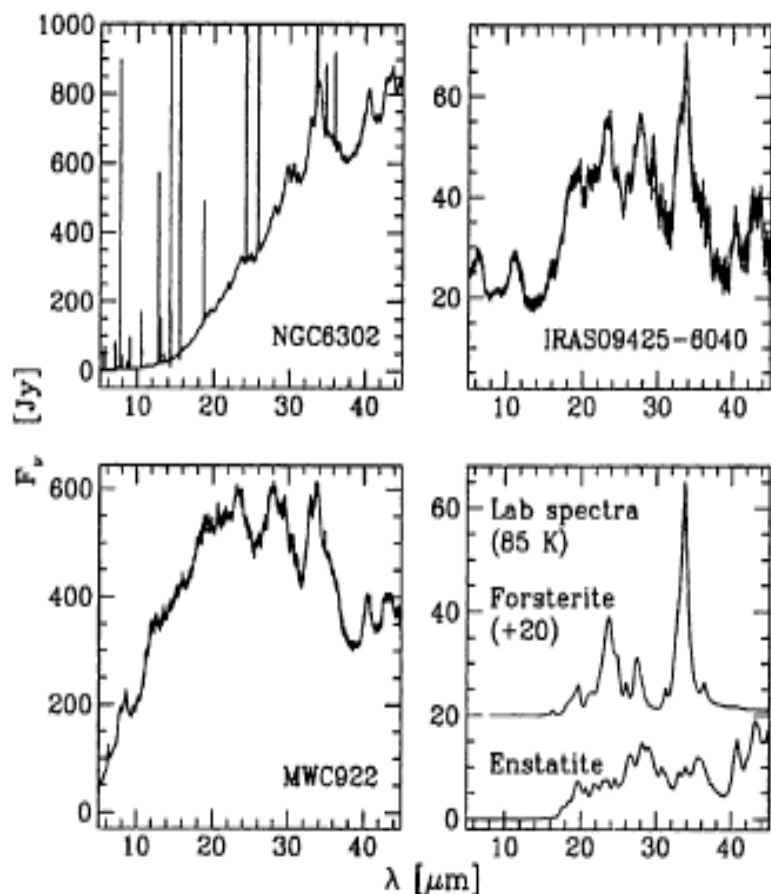


Figure 1. The spectrum of the planetary nebula NGC6302, the AGB star IRAS09425-6040 and the MWC922, which has an unknown evolutionary status, together with the laboratory spectra of forsterite (Mg_2SiO_4) and enstatite ($MgSiO_3$) multiplied with a blackbody of 85 K. The feature at $10\mu m$ in IRAS09425-6040 is due to SiC.

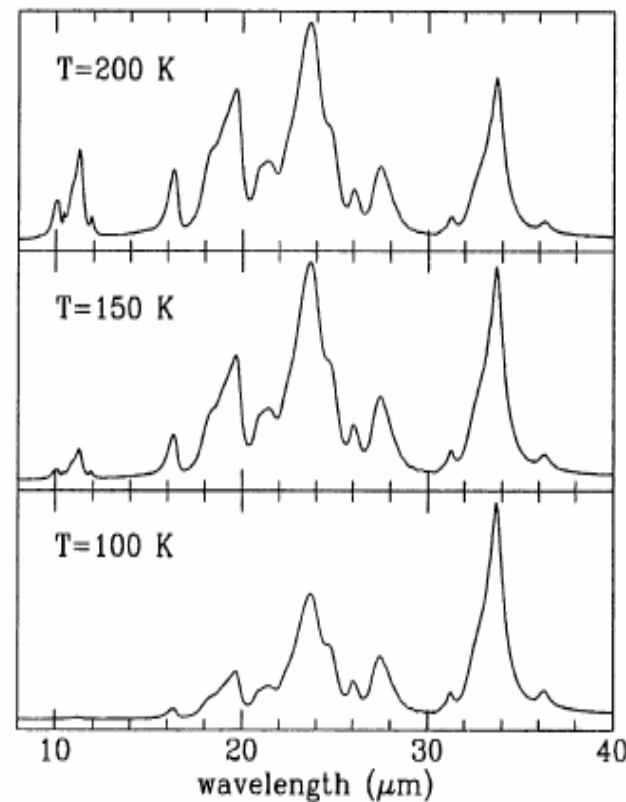


Figure 2. Laboratory transmission spectrum of forsterite, multiplied with blackbody curves of 200, 150 and 100 K. Note the decrease in the strength of the peaks in the $10\mu m$ region when lowering the temperature.

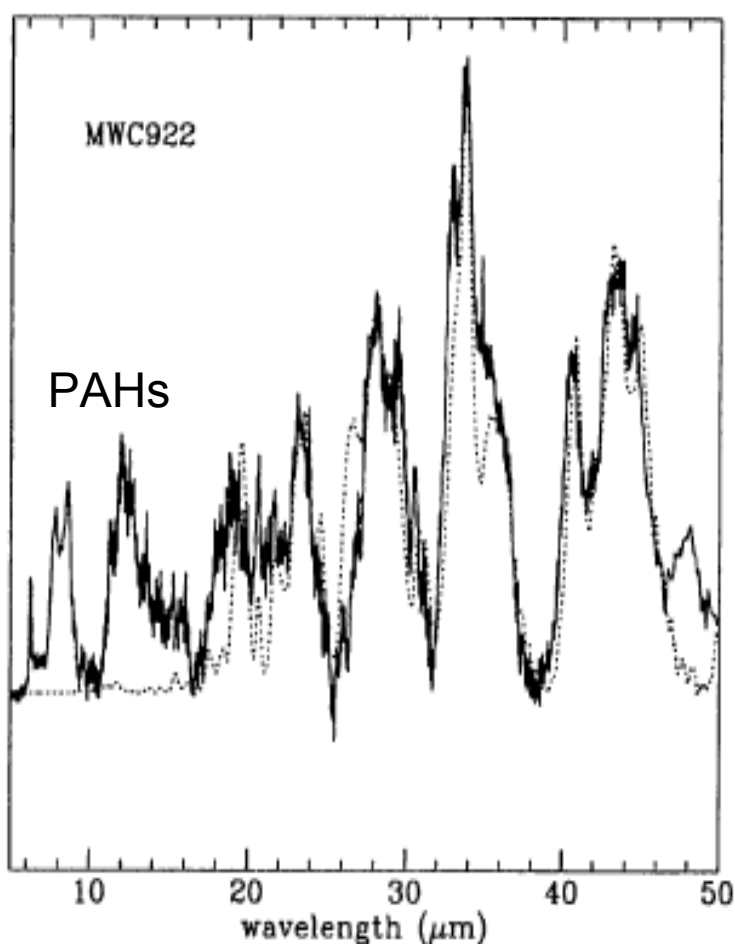


Figure 4. The model fit (dotted line) to the continuum subtracted spectrum of MWC922 (solid line). The derived temperature of the forsterite is respectively 90 and for enstatite (50% clino-enstatite and 50% ortho-enstatite) respectively 100. Note that this two component model already reproduces the observed features rather well. The mismatch at the shortest wavelengths is due to PAH features, which are not incorporated in the model.

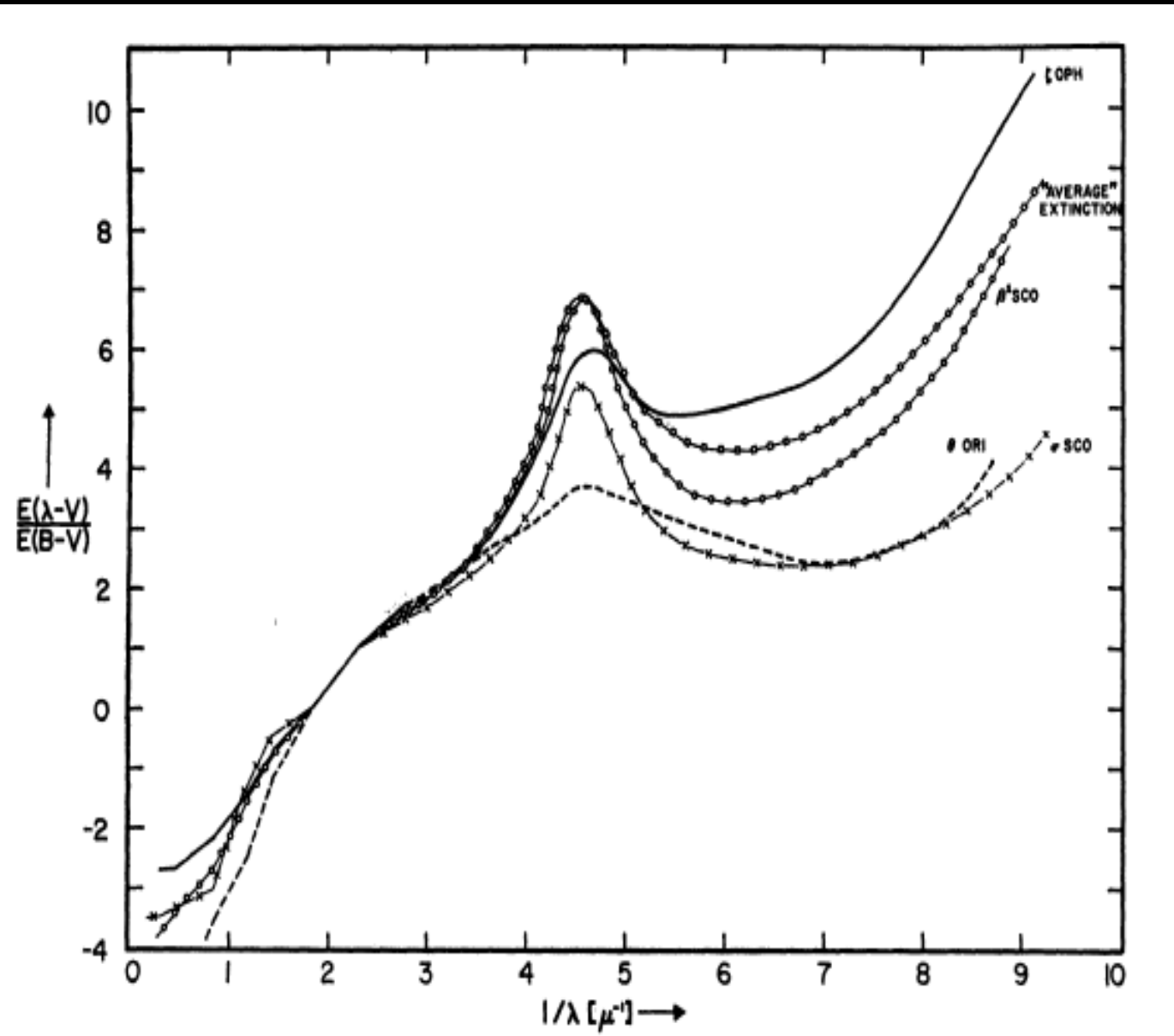
Molster et al. 2000

Dust

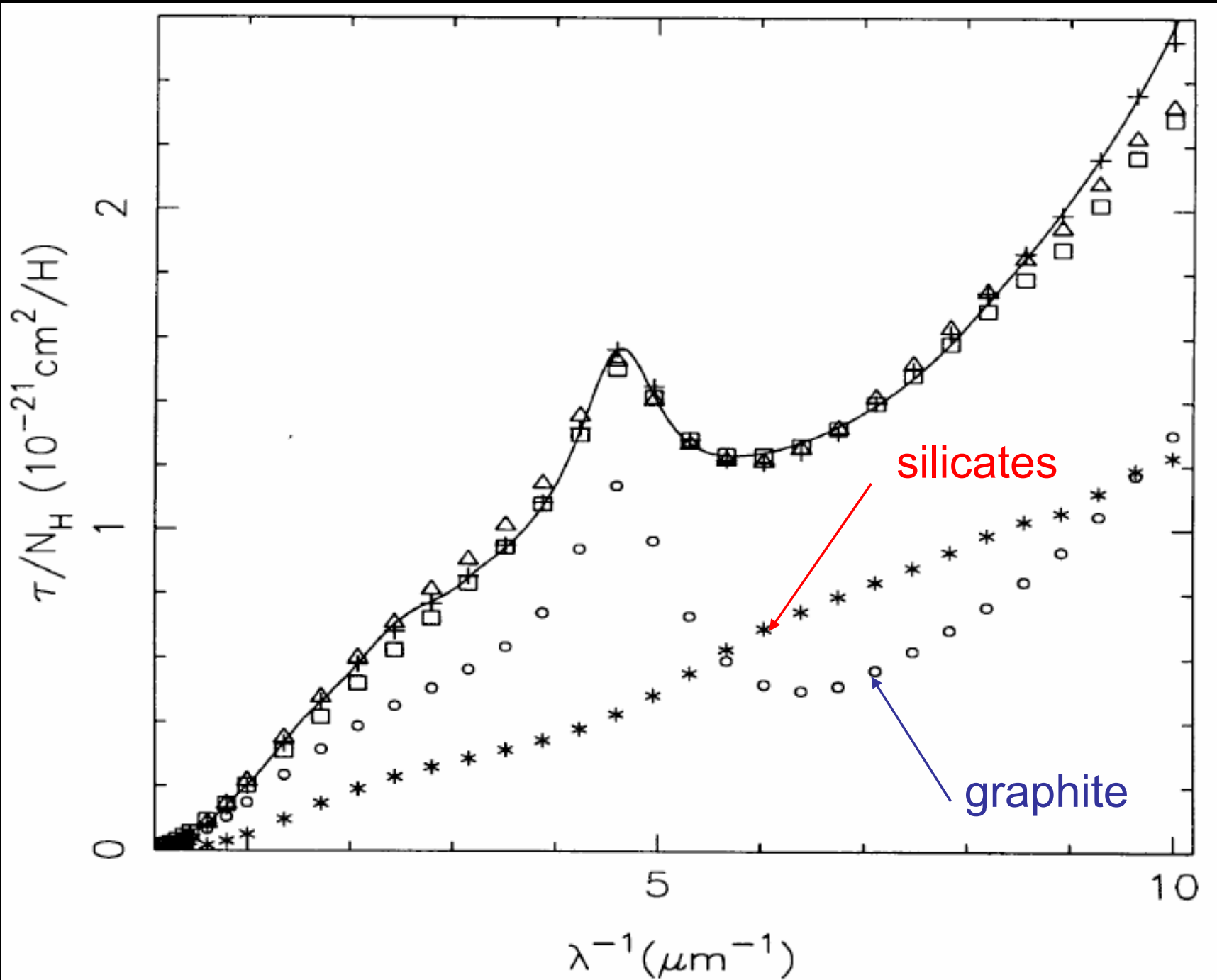
- crystalline silicates
 - fraction crystalline/anorphous ranges from few % to $\sim 50\%$, vs. \leq few % in interstellar clouds

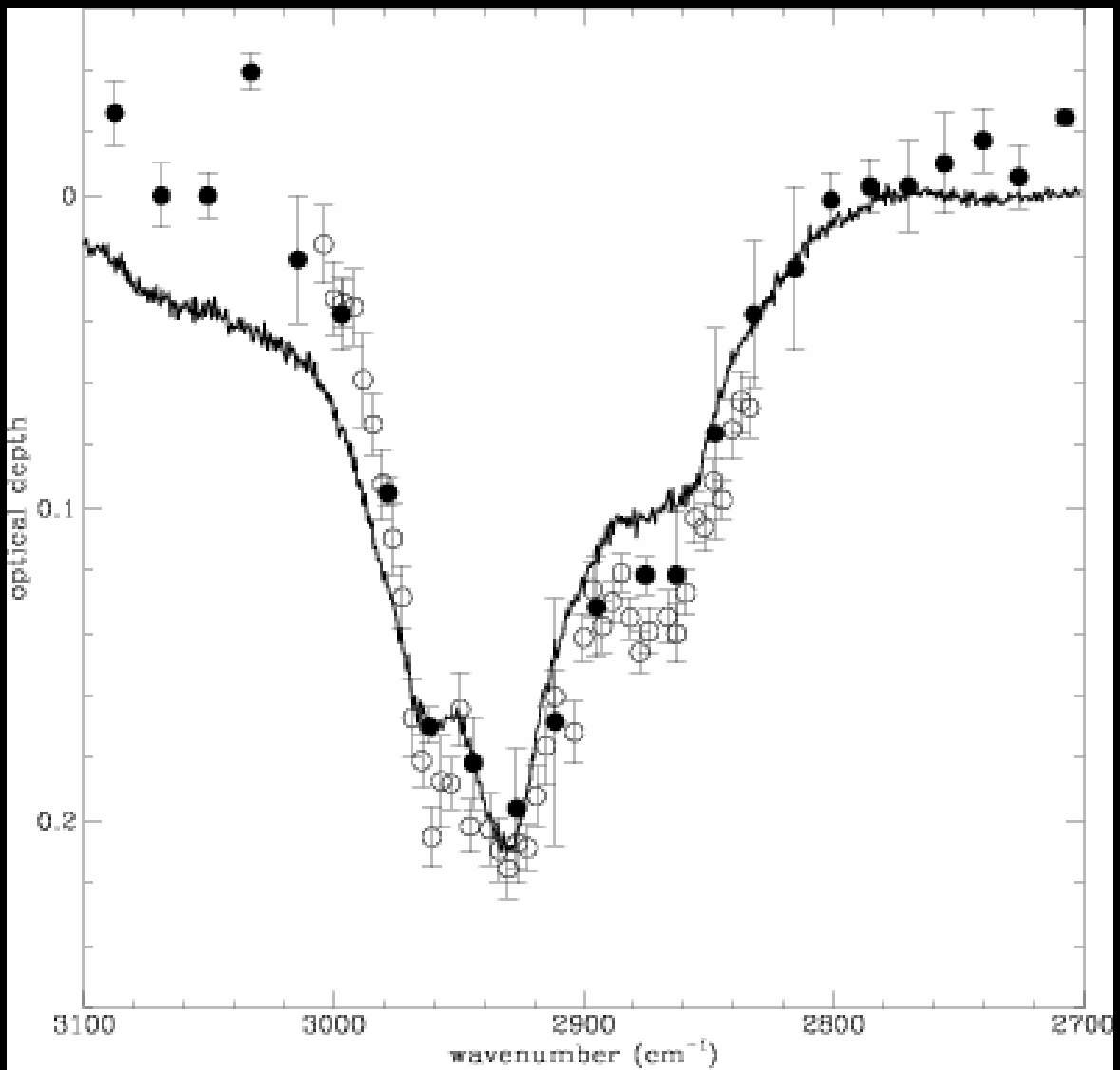
Dust

- carbonaceous material
 - 2175Å extinction bump \Rightarrow ‘graphitic’ material
 - $3.4\mu\text{m}$ absorption diffuse ISM \Rightarrow ‘aliphatic’
 C_H (aliphatic means chain-like, i.e. does not contain ring structures)
 - mass extinction coefficient (opacity) $\Rightarrow \sim 60\%$ of C in solid form



Bless&Savage
1972





Galactic center
source IRS 6E
vs laboratory

Hydrogenated
carbon grains

Mennella et al.
2001

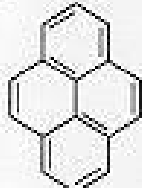
Dust

- PAHs
 - Series of discrete emission bands at 3.29 μm , 6.2 μm , 7.7 μm , 8.6 μm , 11.3 μm , ...
 - best fit by Polycyclic Aromatic Hydrocarbons with 20-100 carbon atoms containing ~1% of carbon abundance.

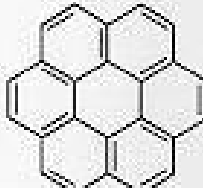
PAH Structures

Pericondensed

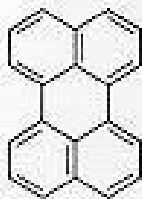
(More than one internal Carbon node)



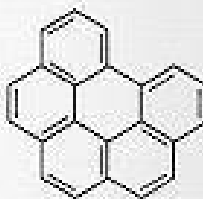
Pyrene
C₁₆H₁₀



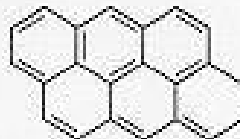
Coronene
C₂₄H₁₂



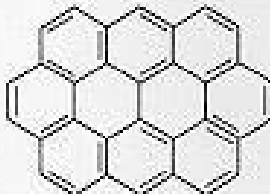
Perylene
C₂₀H₁₂



Benzo[ghi]perylene
C₂₂H₁₂



Antanthrene
C₂₂H₁₂



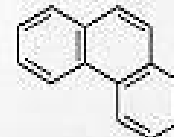
Ovalene
C₃₂H₁₄

Catacondensed

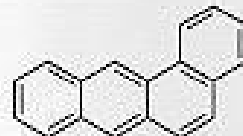
(No internal Carbon vertices)



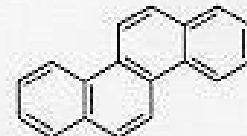
Naphthalene
C₁₀H₈



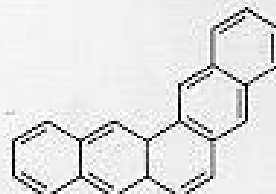
Phenanthrene
C₁₄H₁₀



Tetraphene
C₁₈H₁₂



Chrysene
C₁₈H₁₂



Pentaphene
C₂₂H₁₄



Pentacene
C₂₂H₁₄

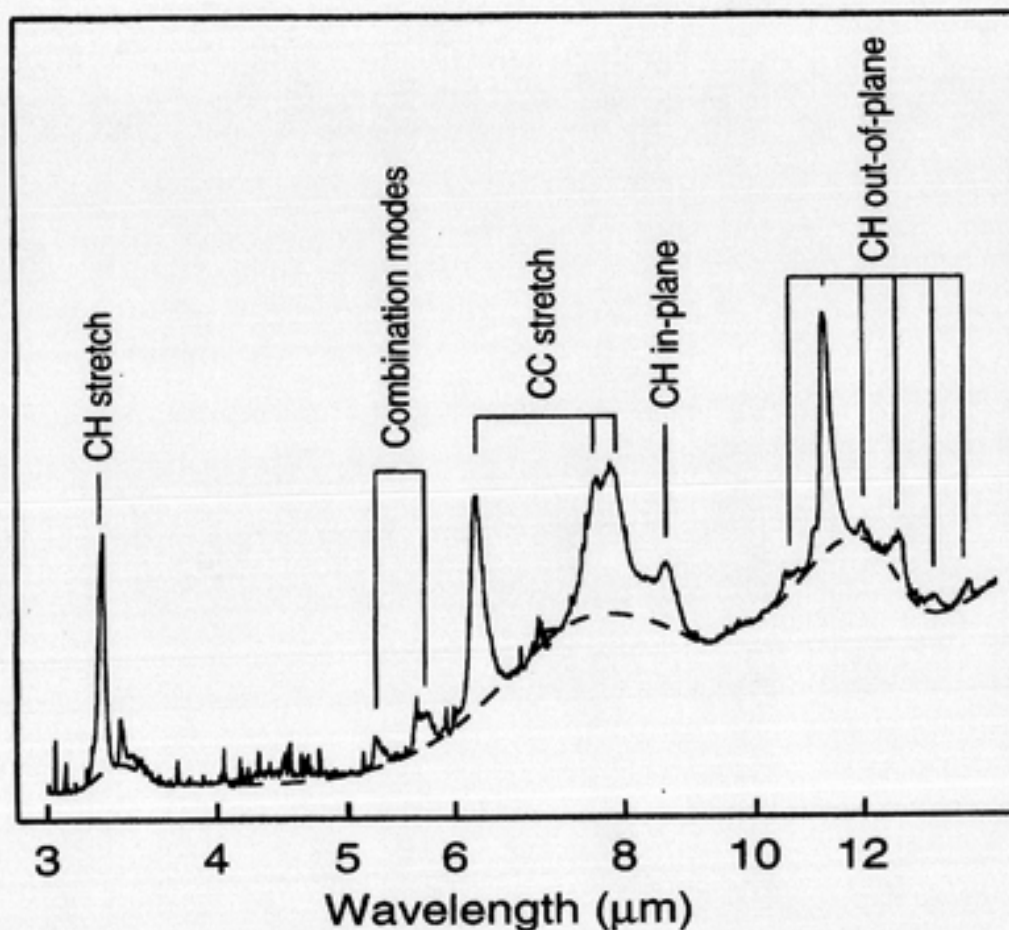
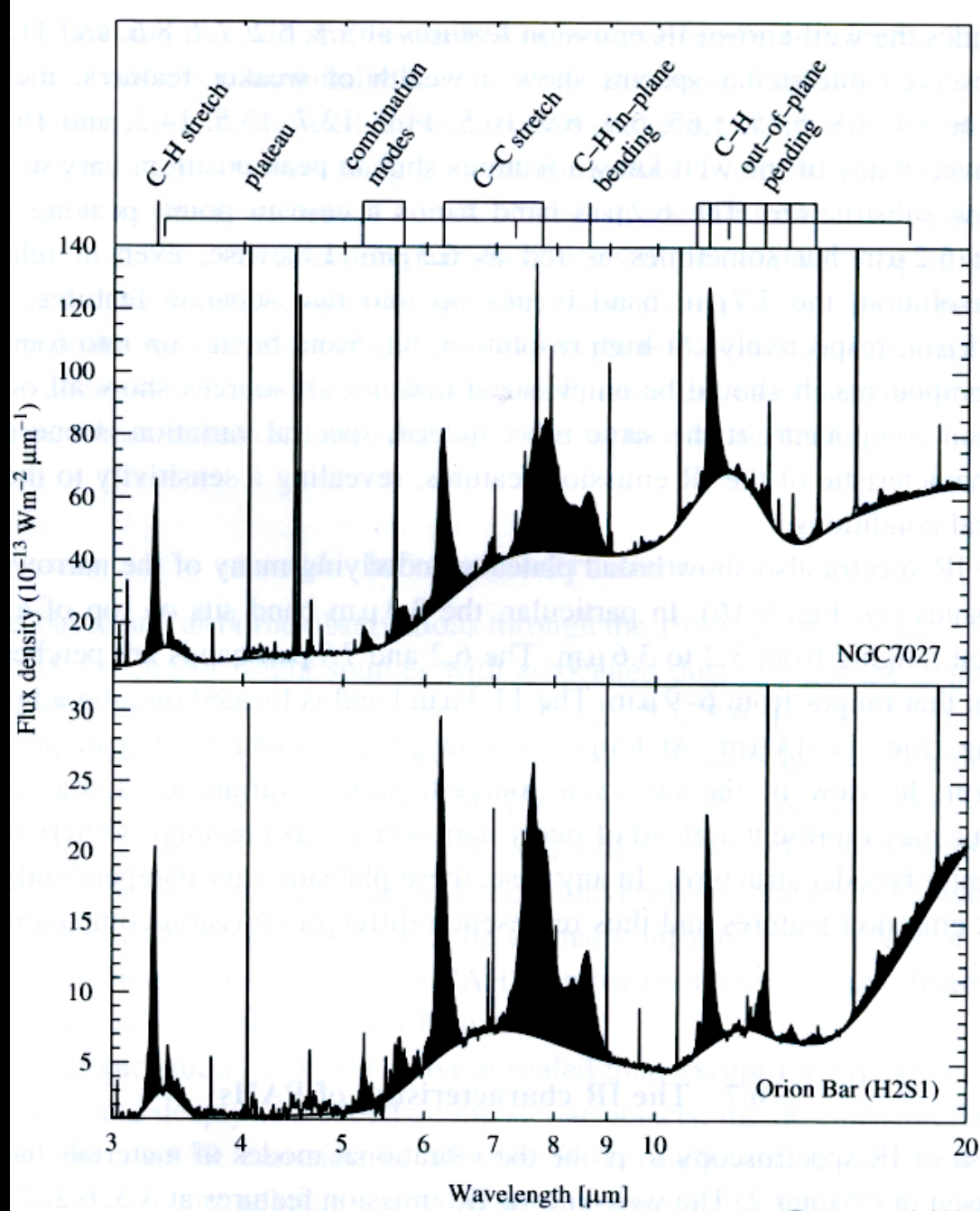


Figure 6.12. Assignment of aromatic features in the spectrum of the planetary nebula NGC 7027 to vibrational modes in PAHs. Figure courtesy of Emma Bakes, adapted from Bakes *et al* (2001).

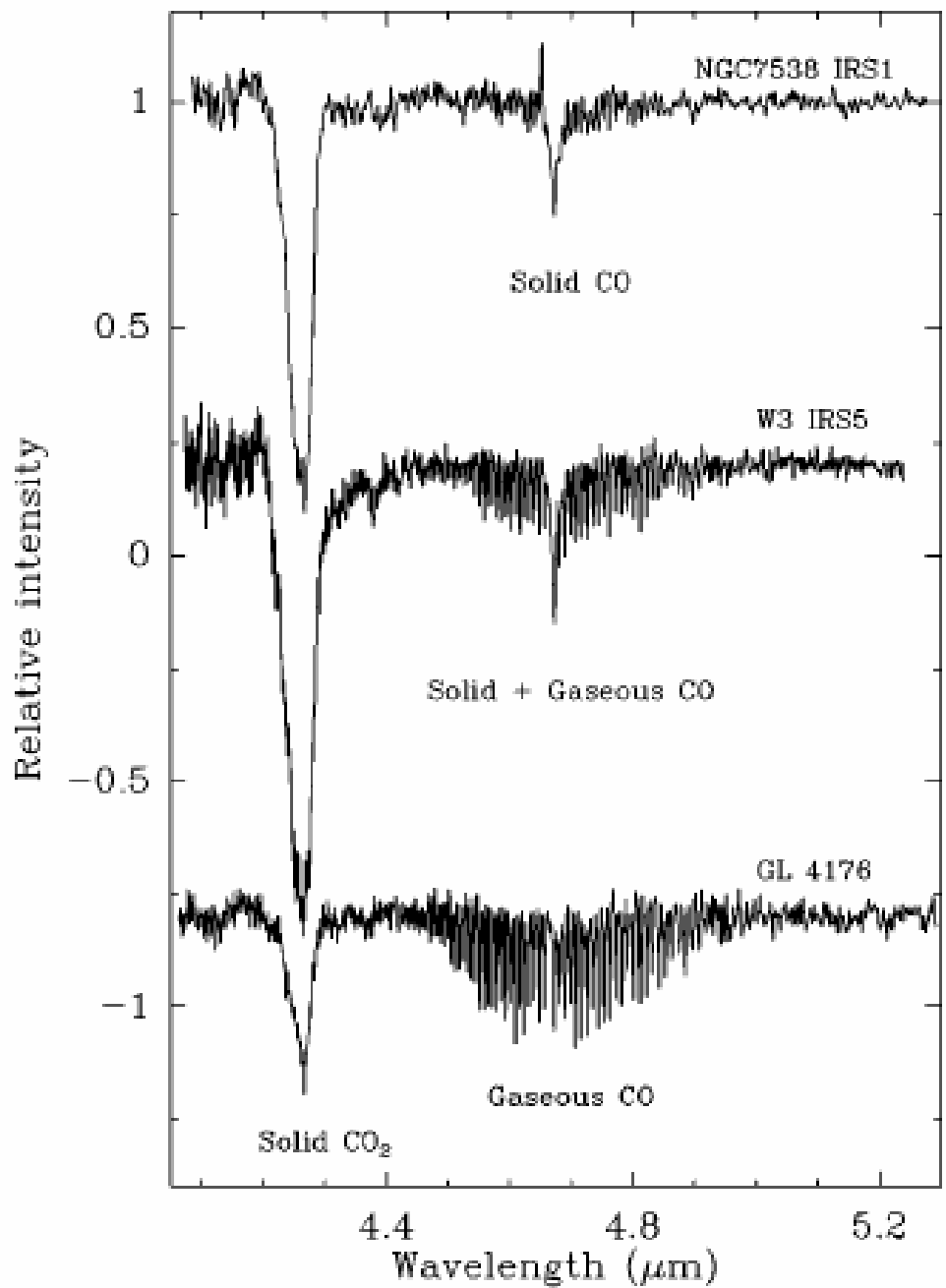
PAH spectral features in IR spectra of NGC7027 (PN) & Orion Bar (PDR)

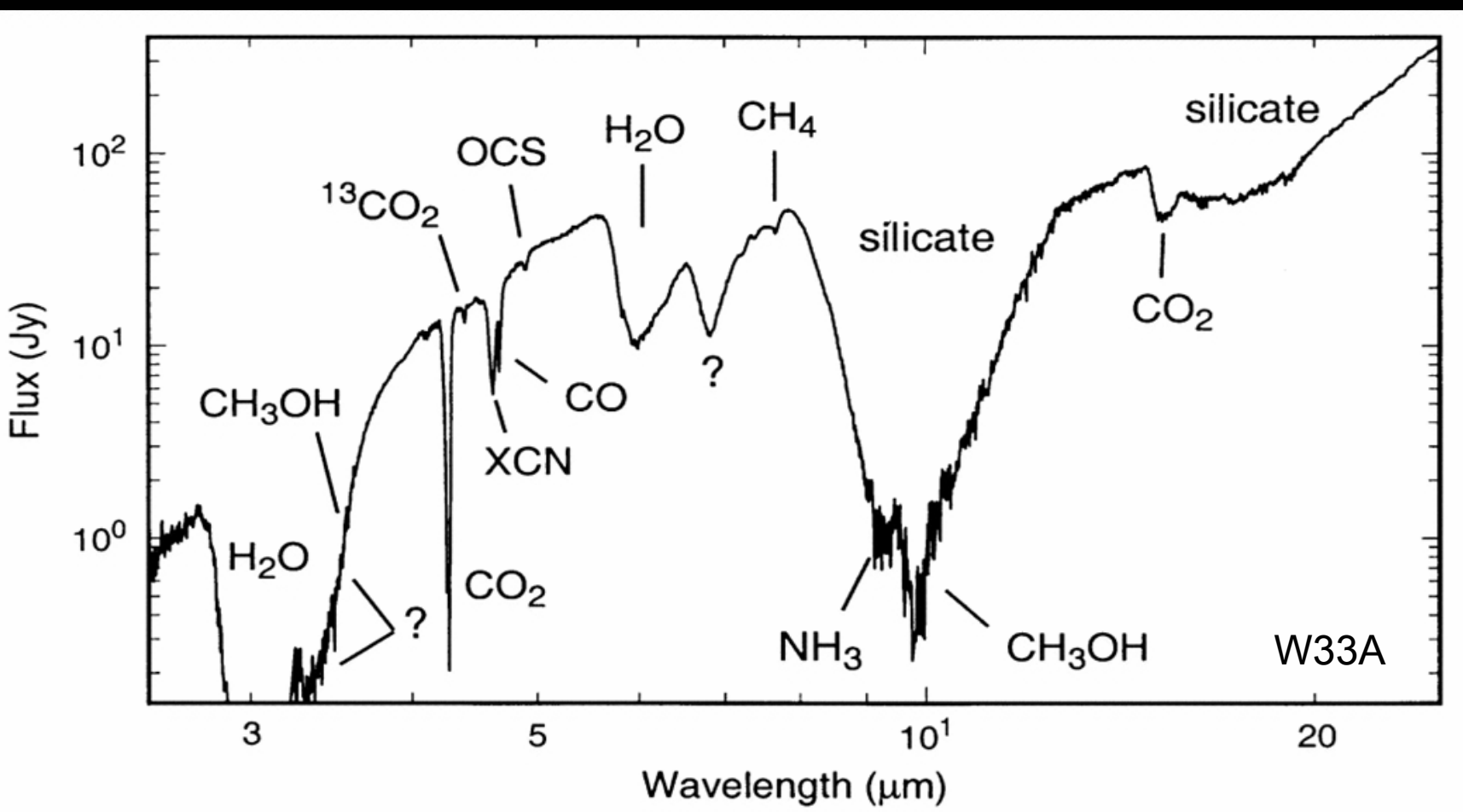


Dust

- Ices
 - discrete absorption features in dense, cold clouds:

3.1, 6.0 μm	H_2O ice
4.27, 15.2 μm	CO_2 ice
4.67 μm	CO ice
3.53, 9.75 μm	CH_3OH ice
7.68 μm	CH_4 ice

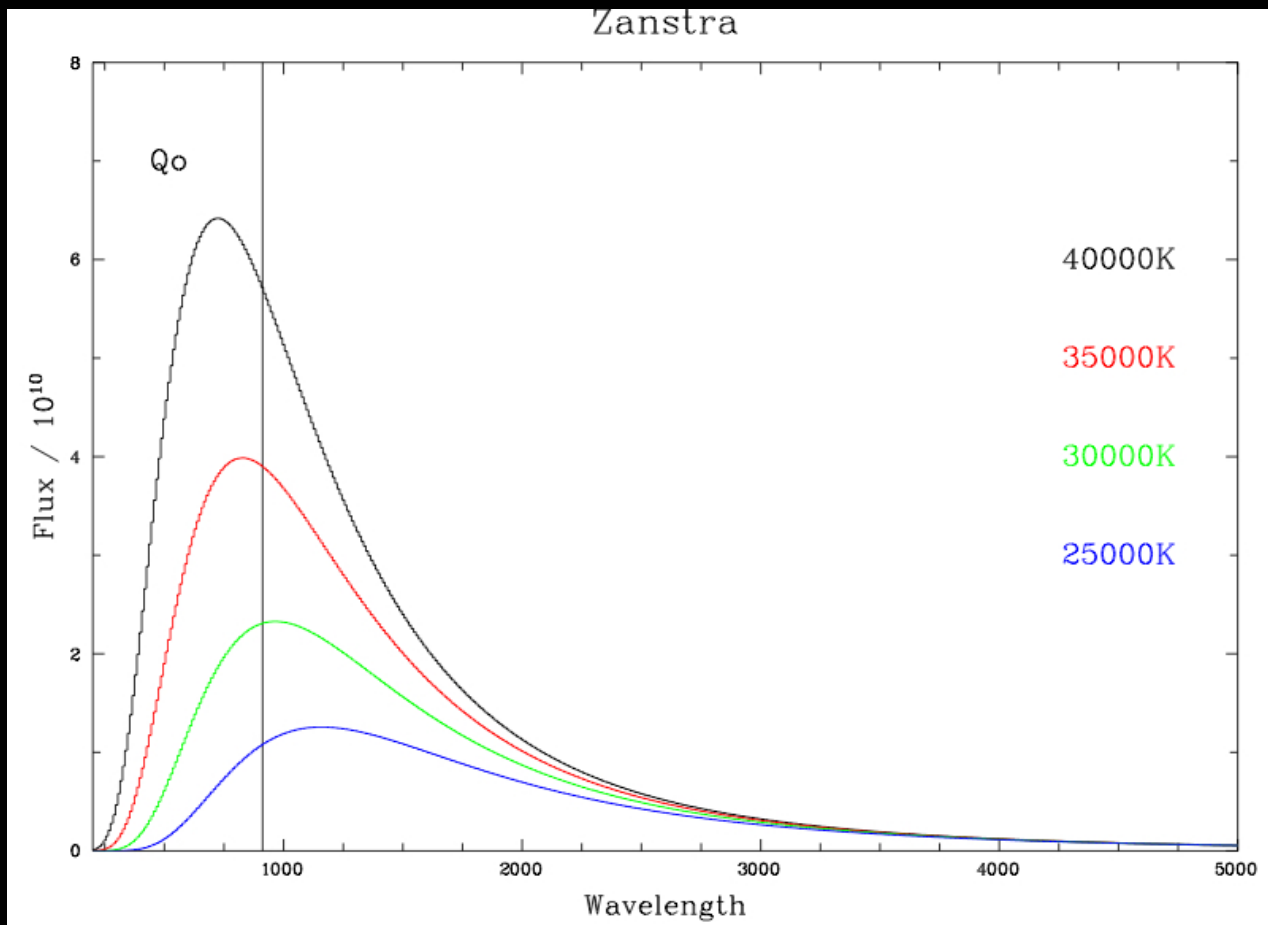




Dust

- Ices
 - ices can be distinguished from gas-phase by:
 - lack of rotational structure bands
 - broadening bands
 - shape of ice bands provides constraints on environmental molecules, e.g.:
 - H₂O-rich ices: “polar” ices
 - H₂O-poor ices: “apolar” ices

Review: Boogert & Ehrenfreund, astro-ph/0311163



Fraction of photons emitted by a star above 13.6eV increases rapidly with stellar temperature from 10^{-10} (Sun), to 10^{-5} (A0V, 10^4 K), 10% (B0V, 3.10^4 K), ~50% (O3V, 5.10^5 K).